

[Master's Projects](#)

[Master's Theses and Graduate Research](#)

Spring 2012

METAMORPHIC WORM THAT CARRIES ITS OWN MORPHING ENGINE

Sudarshan Madenur Sridhara
San Jose State University

Follow this and additional works at: https://scholarworks.sjsu.edu/etd_projects



Recommended Citation

Sridhara, Sudarshan Madenur, "METAMORPHIC WORM THAT CARRIES ITS OWN MORPHING ENGINE" (2012). *Master's Projects*. 240.
DOI: <https://doi.org/10.31979/etd.unb6-nb8s>
https://scholarworks.sjsu.edu/etd_projects/240

This Master's Project is brought to you for free and open access by the Master's Theses and Graduate Research at SJSU ScholarWorks. It has been accepted for inclusion in Master's Projects by an authorized administrator of SJSU ScholarWorks. For more information, please contact scholarworks@sjsu.edu.

METAMORPHIC WORM THAT CARRIES ITS OWN MORPHING ENGINE

A Project

Presented to

The Faculty of the Department of Computer Science

San José State University

In Partial Fulfillment

of the Requirements for the Degree

Master of Science

by

Sudarshan Madenur Sridhara

May 2012

© 2012

Sudarshan Madenur Sridhara

ALL RIGHTS RESERVED

The Designated Project Committee Approves the Project Titled

METAMORPHIC WORM THAT CARRIES ITS OWN MORPHING ENGINE

by

Sudarshan Madenur Sridhara

APPROVED FOR THE DEPARTMENT OF COMPUTER SCIENCE

SAN JOSÉ STATE UNIVERSITY

May 2012

| | |
|-------------------|--------------------------------|
| Dr. Mark Stamp | Department of Computer Science |
| Dr. Chris Pollett | Department of Computer Science |
| Dr. Teng Moh | Department of Computer Science |

ABSTRACT

METAMORPHIC WORM THAT CARRIES ITS OWN MORPHING ENGINE

by Sudarshan Madenur Sridhara

Metamorphic malware changes its internal structure across generations, but its functionality remains unchanged. Well-designed metamorphic malware will evade signature detection. Recent research has revealed techniques based on hidden Markov models (HMMs) for detecting many types of metamorphic malware, as well as techniques for evading such detection.

A worm is a type of malware that actively spreads across a network to other host systems. In this project we design and implement a prototype metamorphic worm that carries its own morphing engine. This is challenging, since the morphing engine itself must be morphed across replications, which imposes significant restrictions on the structure of the worm. Our design also employs previously developed techniques to evade detection. We provide test results to confirm that this worm effectively evades signature and HMM-based detection, and we consider possible detection strategies. This worm provides a concrete example that should prove useful for additional malware detection research.

ACKNOWLEDGEMENTS

I would like to thank Dr. Mark Stamp for trusting me with his idea. His continued support and guidance were the keys to the success of this project.

TABLE OF CONTENTS

CHAPTER

| | | |
|----------|---|-----------|
| 1 | Introduction | 1 |
| 2 | Malware types and detection techniques | 3 |
| 2.1 | Malware types | 3 |
| 2.1.1 | Viruses | 3 |
| 2.1.2 | Worms | 5 |
| 2.2 | Detection techniques | 5 |
| 2.2.1 | Signature-based detection | 5 |
| 2.2.2 | Anomaly-based detection | 6 |
| 2.2.3 | Integrity checkers | 6 |
| 2.2.4 | Hidden Markov Model based detection | 7 |
| 3 | Metamorphic techniques | 8 |
| 3.1 | Register Swap | 8 |
| 3.2 | Subroutine permutation | 8 |
| 3.3 | Garbage Instruction Insertion | 9 |
| 3.4 | Instruction substitution | 9 |
| 3.5 | Transposition | 10 |
| 3.6 | Formal grammar mutation | 10 |
| 4 | Binary similarity | 12 |
| 4.1 | N-gram similarity | 12 |
| 4.2 | Similarity using graph technique | 14 |

| | | |
|----------|---|-----------|
| 4.2.1 | Opcode graphs | 15 |
| 4.2.2 | Similarity Score | 15 |
| 5 | Hidden Markov Models and virus detection | 16 |
| 5.1 | Hidden Markov Models | 16 |
| 5.1.1 | An example | 18 |
| 5.2 | The three problems | 20 |
| 5.2.1 | Forward Algorithm | 20 |
| 5.2.2 | Backward Algorithm | 21 |
| 5.2.3 | Baum-Welch Algorithm | 22 |
| 5.3 | HMMs and Virus detection | 23 |
| 5.3.1 | Log Likelihood Per Opcode | 23 |
| 5.3.2 | Effectiveness of HMM detection | 25 |
| 5.4 | Evading HMM detection | 25 |
| 6 | Design and implementation | 27 |
| 6.1 | Structure | 27 |
| 6.2 | Memory Layout | 29 |
| 6.3 | Metamorphic techniques used | 29 |
| 6.3.1 | Equivalent instruction substitution | 30 |
| 6.3.2 | Dead code insertion | 31 |
| 6.4 | Functionality | 31 |
| 6.5 | Implementation | 33 |
| 6.5.1 | Libraries used | 34 |
| 7 | Experiments | 35 |
| 7.1 | Test data | 35 |

| | | |
|---------------------------|--|-----------|
| 7.2 | N-gram Similarity | 36 |
| 7.3 | Similarity using graph technique | 39 |
| 7.4 | HMM | 40 |
| 8 | Conclusion | 46 |
| 9 | Future work | 47 |
| LIST OF REFERENCES | | 48 |

APPENDICES

| | | |
|----------|--|----|
| A | Equivalent instructions used by the worm | 51 |
| B | Dead code instructions used by the worm | 52 |
| C | Similarity Graphs | 53 |
| D | Additional HMM results | 57 |
| E | Selected HMM Models | 62 |

LIST OF FIGURES

Figure

| | | |
|-----|--|----|
| 3.1 | Subroutine permutation [24] | 9 |
| 3.2 | A simple polymorphic decryptor and two variants [31] | 11 |
| 3.3 | Formal grammar for decrpytor mutation [31] | 11 |
| 4.1 | Similarity based on n-gram analysis [14] | 14 |
| 4.2 | n-gram similarity of two NGVCK viruses [30] | 14 |
| 5.1 | Generic Hidden Markov Model | 17 |
| 5.2 | Extracted opcode sequence | 24 |
| 6.1 | Metamorphic worm components | 28 |
| 6.2 | Metamorphic worm memory layout | 29 |
| 7.1 | Similarity graph MWOR_0 vs MWOR_1 | 39 |
| 7.2 | Similarity using graph technique | 40 |
| 7.3 | HMM with N = 2, padding-ratio: 0.5 | 42 |
| 7.4 | HMM with N = 2, padding-ratio 2.5 | 44 |
| 7.5 | ROC Curves for different padding-ratios | 44 |
| C.1 | Similarity graph - MWOR_1 vs MWOR_2 | 53 |
| C.2 | Similarity graph - MWOR_2 vs MWOR_3 | 54 |
| C.3 | Similarity graph - MWOR_3 vs MWOR_4 | 54 |
| C.4 | Similarity graph - MWOR_4 vs MWOR_5 | 55 |
| C.5 | Similarity graph - MWOR_5 vs MWOR_6 | 55 |

| | | |
|-----|--|----|
| C.6 | Similarity graph - MWOR_6 vs MWOR_7 | 56 |
| D.1 | HMM with N = 3, worm-padding ratio 2.0 | 57 |
| D.2 | HMM with N = 3, worm-padding ratio 3.0 | 58 |
| D.3 | HMM with N = 3, worm-padding ratio 4.0 | 59 |

LIST OF TABLES

Table

| | | |
|-----|---|----|
| 5.1 | Finding HMM optimal state sequence | 19 |
| 6.1 | Equivalent instruction table | 30 |
| 7.1 | Mapping from Benign file ID to actual executable file | 36 |
| 7.2 | Similarity between MWOR files | 37 |
| 7.3 | Similarity between MWOR and benign files | 38 |
| 7.4 | Similarity between BEN files | 38 |
| 7.5 | Similarity using graph technique - MWOR files | 41 |
| 7.6 | Similarity using graph technique - MWOR and BEN files | 41 |
| 7.7 | Similarity using graph technique - BEN files | 42 |
| 7.8 | LLPO scores - padding-ratio: 0.5, N=2 | 43 |
| 7.9 | ROC AUC statistics for different padding-ratios | 45 |
| A.1 | Equivalent instructions used by the worm | 51 |
| B.1 | Dead code instructions used by the worm | 52 |
| D.1 | LLPO scores - Worm-padding ratio: 2.0, N=3 | 59 |
| D.2 | LLPO scores - Worm-padding ratio: 3.0, N=3 | 60 |
| D.3 | LLPO scores - Worm-padding ratio: 4.0, N=3 | 61 |
| E.1 | HMM matrices, N = 2 Worm-padding ratio: 2.0 | 62 |
| E.2 | HMM matrices, N = 3 Worm-padding ratio: 2.0 | 66 |
| E.3 | HMM matrices, N = 2 Worm-padding ratio: 3.0 | 69 |

| | | |
|-----|---|----|
| E.4 | HMM matrices, N = 3 Worm-padding ratio: 3.0 | 72 |
| E.5 | HMM matrices, N = 2 Worm-padding ratio: 4.0 | 75 |
| E.6 | HMM matrices, N = 3 Worm-padding ratio: 4.0 | 78 |

CHAPTER 1

Introduction

Metamorphism is the process of transforming a piece of software into unique instances [20]. In metamorphic software, copies of the software are functionally equivalent but their internal structure differs. Metamorphism is used by virus writers to avoid detection by antivirus software which primarily use signature based detection techniques [2].

Metamorphism provides virus writers the opportunity to develop malware that is undetectable, with respect to static analysis [10]. Therefore, it is natural to expect an increase in volume as well as complexity of metamorphic viruses in the near future.

Although metamorphic viruses have been extensively studied [1, 6, 12, 18, 25, 26, 30], a metamorphic worm presents significant challenges. Metamorphic viruses do not need to carry their own morphing engine. In the case of some highly metamorphic viruses, such as NGVCK [19], the metamorphic generator is separate from the virus body.

Unlike viruses, worms are self-propagating [2], and therefore a metamorphic worm would, most likely, need to carry its own morphing engine. Since the morphing engine itself can act as a signature, a worm that carries its own morphing engine must morph its own morphing engine, as well as the actual worm code, across replications. This presents significant complications and imposes some restrictions on the structure of the morphing engine.

In this paper, we develop and analyze a worm that carries its own morphing engine. That is, the morphing engine morphs itself and the worm across replications.

The resulting metamorphic worms are evaluated based on the lack of similarity between successive generations [14] and their ability to evade detection [30].

CHAPTER 2

Malware types and detection techniques

Malware is a term used to refer to software with malicious functionality.

Malware can exist as an independent executable or infect a benign executable by becoming a part of it. There are different kinds of malware, primarily distinguished from one another by their methods of replication and infection [2].

2.1 Malware types

We discuss two of the most prominent kinds of malware: viruses and worms. Each one of these types is explained in more detail in the sections that follow.

2.1.1 Viruses

A Virus is a malicious piece of code that tries to attach itself to other executable code upon execution. The executable file to which the virus successfully attaches to, is said to be “infected” [2]. Viruses employ numerous methods to escape detection by common detection methods like signature based detection. The most prominent methods used for this purpose are encryption, polymorphism and metamorphism [2].

2.1.1.1 Encrypted viruses

Most of the executable portion of an encrypted virus is encrypted. A small block of decryptor code exists in the virus to decrypt its encrypted body, when the virus is being executed. Encryption using different keys defeats signature based detection by not providing a common signature that can be used to detect the virus.

However, the decryptor remains constant across generations, because of which, the code pattern of the decryptor can be used for detection.

2.1.1.2 Polymorphic viruses

A polymorphic virus is essentially an encrypted virus which changes its decryptor loop across generations. A polymorphic virus, theoretically, has an infinite number of variations of the decryptor loop and therefore, has no common part in the virus body across replications [2].

The most common method to detect polymorphic viruses is code emulation. Although the decryptor changes across replications, the encrypted body will result in the same block of code once decrypted. This enables in memory detection of the virus, once the decryptor has performed the decryption.

2.1.1.3 Metamorphic viruses

Metamorphic viruses do not use encryption and decryptor functions. Instead, the entire body of the virus is changed across generations, while retaining functionality. This produces a new virus body for each replication.

A key component of metamorphic viruses is a mutation engine [15]. The mutation engine is responsible for morphing the body of the metamorphic virus across generations. The mutation engine can be independent of the resultant metamorphic virus, or it can be stored as part of the virus body. In the former case a higher degree of metamorphism can be achieved because the mutation engine itself need not be morphed. In the latter case, the mutation engine itself needs to be morphed across generations. This places restrictions on the structure of the mutation engine, and also the level of metamorphism that can be achieved using it [7, 28].

Some of the morphing techniques employed by metamorphic viruses are explained in more detail in the Chapter 3.

2.1.2 Worms

Like viruses, worms are self-replicating malware. However, there are several characteristics that distinguish a worm from a virus.

Firstly, worms are standalone [2]. They do not rely on a host executable to which they need to attach to. Secondly, unlike viruses which only replicate and infect executable programs within their host machine, worms spread from host to host across the network. Worms also operate without human intervention [22].

Similar to viruses, worms can employ different techniques to avoid signature based detection. Polymorphism and metamorphism have been employed by worms [3, 7].

2.2 Detection techniques

As viruses continue to evolve, there has been a corresponding evolution in virus detection technologies as well. This section presents some techniques that antivirus software most commonly employ. Some niche techniques are also presented.

2.2.1 Signature-based detection

Signature-based detection is by far, the most commonly used technique for virus detection [23]. A signature comprises of sequences of bytes extracted from a virus, which can be used to uniquely identify the virus. A signature scanner scans executable files for such signatures, using a database of virus signatures [2]. If a

match occurs, the executable is assumed to be infected by the virus corresponding to the matching signature.

Signature scanning is implemented using algorithms that can be used to scan for a large number of signatures quickly. However, there are several drawbacks in signature based detection. To be able to detect new virus, a signature needs to be extracted from the virus and added to the signature database. Also, signature based scanning is easily defeated by using techniques like polymorphism and metamorphism [23].

2.2.2 Anomaly-based detection

Heuristic methods can be employed by anti-virus software to detect anomalous behavior, instead of looking for specific virus signatures. Heuristic methods can be either static or dynamic. Static heuristics involve static code analysis to look for suspicious structures like decryption loops, self-modifying code, use of undocumented API calls, manipulation of interrupt vectors, etc. [2, 27].

Dynamic heuristic methods determine whether an executable is infected by analyzing its behavior while it is running. Common dynamic methods are behavior monitoring and code emulation [27].

Anomaly-based detection systems can provide protection against zero-day attacks by detecting even unknown viruses. However, anomaly-based detection systems have much higher false positive and false negative rates compared to other detection methods [9].

2.2.3 Integrity checkers

Integrity checkers detect changes to files by comparing their check-sum to their original check-sum stored in a white list. Viruses, with very few exceptions,

operate by changing files. Integrity checkers watch for unauthorized file modifications to determine virus like behavior [4].

2.2.4 Hidden Markov Model based detection

Hidden Markov Models (HMMs) are statistical models, widely used in many problems involving pattern recognition. In the past few years, considerable research has been done on the use of Hidden Markov Models for metamorphic virus detection. A method to detect metamorphic viruses is presented in [30]. It involves training an HMM with opcode sequences extracted from viruses belonging to a certain family. This trained HMM is then used to score other executable files, to check whether they belong to the same virus family. A detailed explanation of the process is given in Section 5.2.

CHAPTER 3

Metamorphic techniques

The metamorphic worm described in this paper makes use of morphing techniques like equivalent instruction substitution and dead code insertion. Apart from these two techniques, there are a number of other morphing techniques employed by metamorphic malware. These techniques may be as elementary as equivalent instruction substitution, or as advanced as formal grammar mutation.

Some of the metamorphic techniques presented in [2] and [3] are explained in this section.

3.1 Register Swap

Register swap is a simple metamorphic technique. It mutates the virus body by swapping the operand registers with different registers. For example, `POP ECX` might be replaced with `POP EBX`, if it is permissible. Opcode sequence remains the same using this technique.

3.2 Subroutine permutation

In this technique changes in the structure of a virus is obtained by reordering the virus' subroutines. If a virus has n different subroutines, then it can generate n -factorial different generations without repeats. Viruses which only use this method may be detected matching multiple short signatures in the same binary. An example of one such permutation is shown in Figure 3.1.

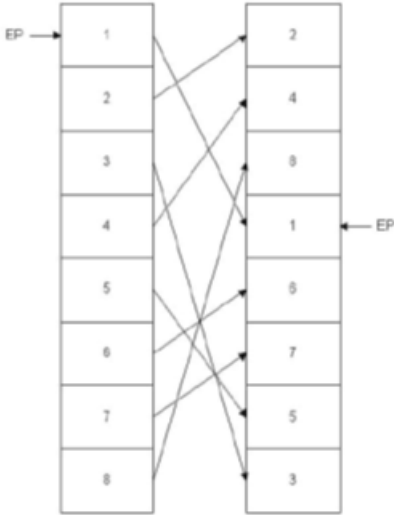


Figure 3.1: Subroutine permutation [24]

3.3 Garbage Instruction Insertion

Garbage instructions are instructions are of two types:

- (1) Instructions that are either not executed
- (2) Instructions that have no effect.

By adding garbage instructions, a virus can potentially generate an unlimited number of unique copies. Examples of instructions that have no effect include NOP, ADD EAX, 0, etc. Such instructions can contribute greatly to metamorphism.

3.4 Instruction substitution

This involves substituting a single instruction or a group of instructions with another instruction or a group of instructions with the same functionality. For instance, MOV R1, R2 is equivalent to PUSH R1 followed by POP R2.

3.5 Transposition

Transposition involves instruction re-ordering. If instructions have no dependency between them, their order of execution can be changed without any change in the overall functionality of the program. For example, instructions:

```
1: ADD [Op1], [Op2]  
2: ADD [Op3], [Op4]
```

can be re-ordered as shown below without any resultant change in functionality.

```
1: ADD [Op3], [Op4]  
2: ADD [Op1], [Op2]
```

The same is true for groups of instructions which have no dependency on one another. This helps to evade signature based detection, as the order of instruction bytes change in the morphed executable.

3.6 Formal grammar mutation

Formal grammar mutation is a formalization of many existing morphing techniques [3, 8, 31]. Classical morphing engines can be viewed as non-deterministic automata, since transitions are possible from every symbol to every other symbol [31], where the symbol set is the set of all possible instructions. In other words, any instruction can be followed by any other instruction. By formalizing mutation techniques, one can apply formal grammar rules and create viral copies with great variation.

Figure 3.2 illustrates a simple polymorphic decryptor template and two possible mutations of the decryptor code achieved using the formal grammar shown

in Figure 3.3. With this decryptor template and formal grammar combination, it is possible to generate 960 different decryptors [31].

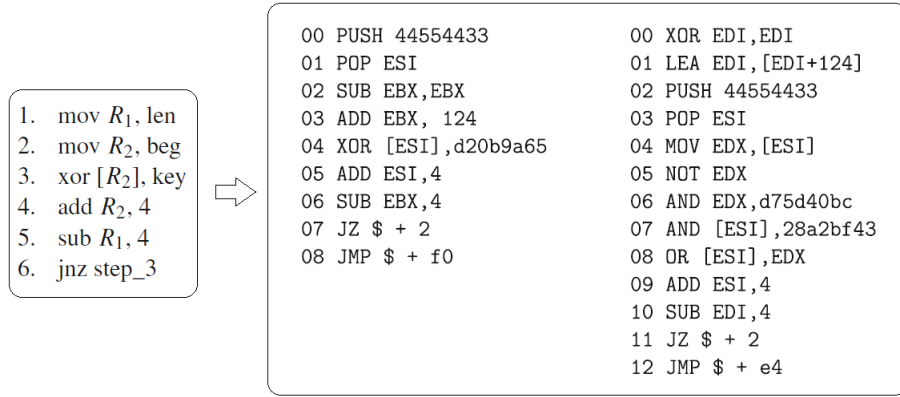


Figure 3.2: A simple polymorphic decryptor and two variants [31]

$$\begin{aligned}
 A &\rightarrow XB \\
 B &\rightarrow Y_4\epsilon \\
 X &\rightarrow X_1X_2|X_2X_1 \\
 X_1 &\rightarrow GX_1|mov R_1, len|push len \oplus pop R_1|xor R_1, \\
 &\quad R_1 \oplus lea R_1, [R_1 + len]|sub R_1, R_1 \oplus add R_1, len \\
 X_2 &\rightarrow GX_2|mov R_2, beg|push beg \oplus pop R_2|xor R_2, \\
 &\quad R_2 \oplus lea R_2, [R_2 + beg]|sub R_2, R_2 \oplus add R_2, beg \\
 Y_4 &\rightarrow GY_4|W_1|S_4W_4 \\
 W_1 &\rightarrow GW_1|xor [R_2], key H_1 \\
 W_1 &\rightarrow not [R_2] \oplus xor [R_2], key \oplus not [R_2] H_1 \\
 W_1 &\rightarrow mov R_3, [R_2] \oplus not R_3 \oplus and R_3, key \oplus and [R_2], \\
 &\quad \neg key \oplus or [R_2], R_3 H_1 \\
 H_1 &\rightarrow GH_1|add R_2, 4 H_2|sub R_2, -4 H_2 \\
 S_4 &\rightarrow GS_1|sub R_2, 4|add R_2, -4 \\
 W_2 &\rightarrow GW_2|xor [R_1][R_2], key H_2 \\
 W_2 &\rightarrow not [R_1][R_2] \oplus xor [R_1][R_2], key \oplus not [R_1][R_2] H_2 \\
 W_2 &\rightarrow mov R_3, [R_1][R_2] \oplus not R_3 \oplus and R_3, key \oplus and \\
 &\quad [R_1][R_2], \neg key \oplus or [R_1][R_2], R_3 H_2 \\
 H_2 &\rightarrow GH_2|sub R_1, 4 \oplus jnz xxx|sub R_1, 4 \oplus jz yyy \oplus jmp xxx \\
 H_2 &\rightarrow add R_1, -4 \oplus jnz xxx|add R_1, -4 \oplus jz yyy \oplus jmp xxx \\
 H_2 &\rightarrow sub ecx, 3 \oplus loop xxx \Leftrightarrow R_1 \equiv ecx
 \end{aligned}$$

Figure 3.3: Formal grammar for decryptor mutation [31]

CHAPTER 4

Binary similarity

The ability of the metamorphic worm described in this paper to evade signature-based detection, is evaluated by analyzing the similarity between various generations of the worm.

4.1 N-gram similarity

In [14], an n-gram based similarity measure is proposed and analyzed. This method can be used to compare sequences of instructions in two assembly program files [12, 30]. This method calculates a score that represents the percentage of similarity between the two files. The method is summarized below:

- (1) Extract instruction opcodes from the two given assembly programs X and Y. Let the length of the extracted opcode sequences from programs X and Y be ‘m’ and ‘n’ respectively. Assign numbers in a sequence to the extracted opcodes: 1 to the first opcode, 2 to the second opcode, etc.
- (2) For all opcode sub-sequences of length three from X’s opcode sequence, check if corresponding sub-sequences occur in the opcode sequence extracted from Y. If a match occurs, (x, y) will be marked on a graph where, x is the position of the first opcode of the matching sub-sequence in Xs opcode sequence, and y is the position of the first opcode in the matching sub-sequence in Y’s opcode sequence.
- (3) After matching all opcode sequences, an $m \times n$ graph is plotted on which all matching sub-sequences are marked. The x-axis corresponds to the opcode

numbers extracted from X and the y-axis corresponds to the opcode numbers extracted from Y. Retain only those line segments on the graph whose length is above a certain threshold value (say five). This is done to eliminate random matches and noise.

- (4) Since a sequential match is done between both sequences, matching sequences of opcodes result in line segments that are parallel to the diagonal ((0,0), (m,n)). If the matching sequence occurs in the same starting location in both opcode sequences, the resulting line segment will fall on the diagonal. If the matching sequence occurs at different starting locations in both opcode sequences, the resulting line segment will be parallel to the diagonal.
- (5) For each axis, calculate the sum of the number of opcodes that are covered by one or more of the line segments retained in (3). This sum is divided by the total number of opcodes on the corresponding axis to find the percentage of match for the assembly program represented by the axis. The final similarity score is the average of the similarity percentage calculated for both axes.

The method summarized above is illustrated graphically in Figure 4.1.

This n-gram based similarity measure is used both in [30] and [12], to compare the similarity between assembly programs that are obtained by disassembling benign files of viruses belonging to the NGVCK family.

An example comparison between two virus files, generated by the NGVCK metamorphic generator [19], presented in [30] is shown in Figure 4.2. The left part of the graph shows matching sub-sequences without eliminating noise. The right

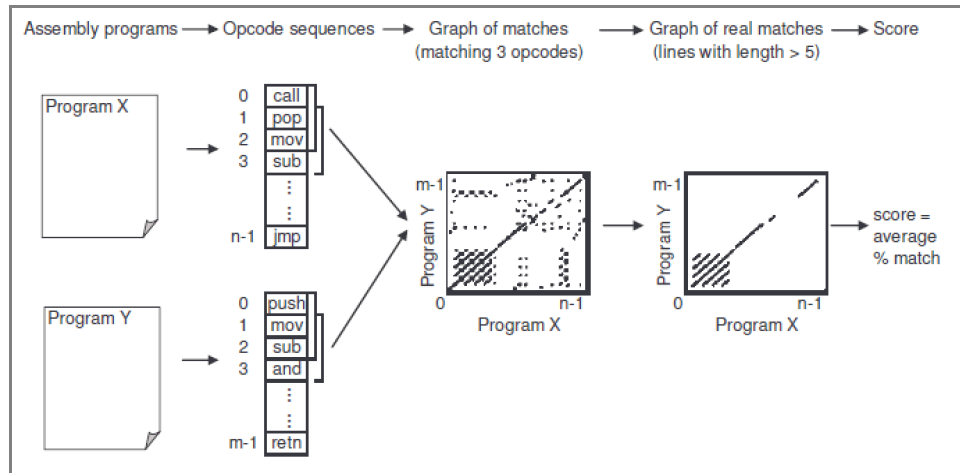


Figure 4.1: Similarity based on n-gram analysis [14]

part shows matching sub-sequences retained after eliminating noise. The final similarity score in this particular instance is 21%.

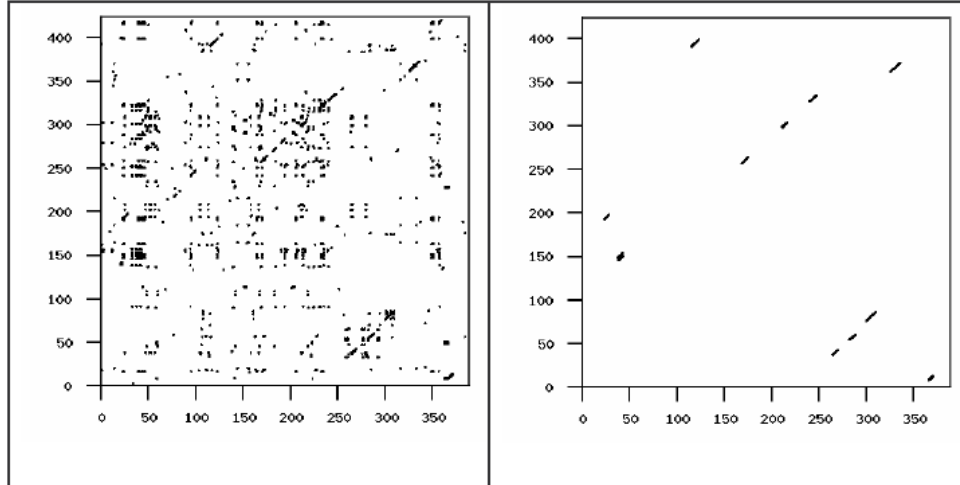


Figure 4.2: n-gram similarity of two NGVCK viruses [30]

4.2 Similarity using graph technique

A method for measuring similarity between executable files using opcode graphs is presented in [18]. This method involves creating weighted directed graphs

using opcodes extracted from executable files. We now summarize the methods used to generate opcode graphs, and to compute similarity using these generated graphs.

4.2.1 Opcode graphs

Each opcode that appears in an executable file's extracted opcode sequence is a node in the directed graph. A directed edge is inserted from this node to every other node corresponding to the successor opcodes. Edge weights represent the transition probabilities to successor nodes.

Counts for opcode pairs are tabulated from the extracted opcode sequence to form a matrix. For each opcode, the counts are converted to probabilities by dividing the count for a digram by the row sum. The resulting matrix is an opcode graph that represents the program using which it was created.

4.2.2 Similarity Score

Let N be the number of distinct opcodes. The opcodes are mapped to numbers 0 to $N - 1$. Let A and B be the opcode graphs for the executable files in question. Elements of the matrices A and B are represented by a_{ij} and b_{ij} respectively.

To compare the matrices, the similarity score $S(A, B)$ is computed using the following scoring function:

$$S(A, B) = \frac{1}{N^2} \left(\sum_{i,j=0}^{N-1} |a_{ij} - b_{ij}| \right)^2$$

If A is the same as B , then the minimal score of 0 is obtained. On the other hand, if $a_{ij} = 1$ and $b_{ik} = 1$ with $j \neq k$, the maximum possible row sum of 2 is obtained. If this maximum row sum is obtained for each row, $S(A, B) = 4$. Therefore, $0 \leq S(A, B) \leq 4$.

CHAPTER 5

Hidden Markov Models and virus detection

Over the past few years, there has been significant research on the use of Hidden Markov Models (HMMs) for metamorphic virus detection [1, 6, 12, 18, 25, 26, 30]. A method is presented in [30] in which an HMM is trained using sequences of opcodes from viruses that belong to a particular family. This trained HMM is then used to score binaries, to determine whether the binaries are viruses that belong to the same family. A threshold can be obtained based on the Log Likelihood Per Opcode (LLPO) score for viruses and benign binaries, which is used to categorize new binaries as viruses or benign binaries based on their LLPO score. This section explains how HMMs work and the way HMMs can be used in virus detection.

5.1 Hidden Markov Models

A Hidden Markov Model (HMM) is a statistical model used to model a Markov process whose states are unknown [21]. Some HMM notations are now presented. The notations presented here are based on the notations used in [21]:

$T \rightarrow$ Length of the observation sequence

$N \rightarrow$ Number of states in the model

$M \rightarrow$ Number of observation symbols

$Q \rightarrow \{q_0, q_1, \dots, q_{N-1}\}$ – Number of observation symbols

$V \rightarrow \{0, 1, \dots, M - 1\}$ – Set of possible observations

$A \rightarrow$ state transition probabilities

$B \rightarrow$ observation probability matrix

$\pi \rightarrow$ initial state distribution

$O \rightarrow (O_0, O_1, \dots, O_{T-1})$ – observation sequence

Figure 5.1 illustrates a generic HMM. The state of the HMM and the observation at time t are represented by X_t and O_t respectively. The initial state X_0 and the A matrix determine the hidden Markov process which is represented in the figure by the portion on top of the dotted line.

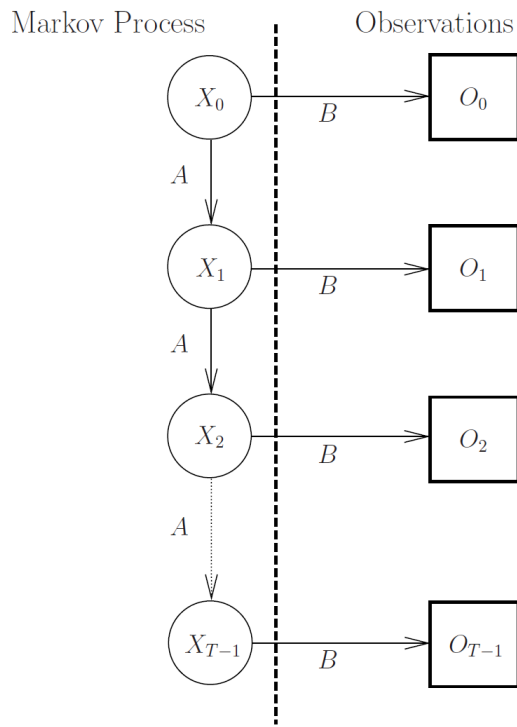


Figure 5.1: Generic Hidden Markov Model

First, the HMM is trained using input data that the HMM needs to represent. Each individual element in the training data maps to an observation symbol. Unique observation symbols are extracted from the set of observations. The trained

model will then be used to determine if a given new sequence of observations is a pattern similar to the one represented by the model.

5.1.1 An example

Here we illustrate the inner workings of an HMM using a simple example [17]. A genie is sitting behind a curtain with urns U_0 , U_1 and U_2 , each containing balls colored red, green and blue in different proportions. Balls colored red, green and blue are indicated by R , G and B respectively. The color of the ball chosen by the genie, at any point of time, is governed by a Markov process unknown to the observer. The observer can only see the color of the chosen ball.

The objective is to predict the urn from which the balls are retrieved based on the order and color of the balls drawn from them. In this example, U_0 , U_1 and U_2 are the states. The possible observations are R , G and B .

The transition probabilities from each state to every other state are represented by matrix A as shown below:

$$A = \begin{matrix} & U_0 & U_1 & U_2 \\ \begin{matrix} U_0 \\ U_1 \\ U_2 \end{matrix} & \left[\begin{array}{ccc} 0.1 & 0.4 & 0.5 \\ 0.6 & 0.2 & 0.2 \\ 0.5 & 0.2 & 0.3 \end{array} \right] \end{matrix}$$

The probability of observations for each of the states is represented by the B matrix as shown below:

$$B = \begin{matrix} & R & G & B \\ \begin{matrix} U_0 \\ U_1 \\ U_2 \end{matrix} & \left[\begin{array}{ccc} 0.5 & 0.3 & 0.2 \\ 0.2 & 0.6 & 0.2 \\ 0.1 & 0.3 & 0.6 \end{array} \right] \end{matrix}$$

Also, the initial probability distribution is represented by the π matrix as shown below:

$$\pi = \begin{bmatrix} 0.4 & 0.3 & 0.3 \end{bmatrix}$$

The matrices π , A and B are row-stochastic; i.e, each row sums up to 1. Each row represents a probability distribution. Now, given a sequence of observations $O = (R, B)$, the objective is to find the most likely state sequence, given the model λ .

In the HMM sense, the most likely state sequence is calculated choosing the state for which the sum of probabilities over all possible state sequences is the highest for each observation. This process is illustrated in Table 5.1. In this case, the optimal state sequence in the HMM sense is U_0U_2 .

Table 5.1: Finding HMM optimal state sequence

| State sequence probabilities | | |
|------------------------------|-------------|------------------------|
| State | Probability | Normalized probability |
| U_0U_0 | 0.0040 | 0.0376 |
| U_0U_1 | 0.0160 | 0.1504 |
| U_0U_2 | 0.0600 | 0.5639 |
| U_1U_0 | 0.0072 | 0.0677 |
| U_1U_1 | 0.0024 | 0.0226 |
| U_1U_2 | 0.0072 | 0.0677 |
| U_2U_0 | 0.0030 | 0.0282 |
| U_2U_1 | 0.0012 | 0.0113 |
| U_2U_2 | 0.0054 | 0.0508 |

| HMM probabilities | | |
|-------------------|---------|--------|
| | Element | |
| | 1 | 2 |
| $P(U_0)$ | 0.7519 | 0.1335 |
| $P(U_1)$ | 0.1580 | 0.1843 |
| $P(U_2)$ | 0.0903 | 0.6824 |

5.2 The three problems

The following three problems can be solved efficiently using HMMs [21].

- (1) Given $\lambda = (A, B, \pi)$ and O , the observation sequence, find $P(O|\lambda)$.
- (2) Given $\lambda = (A, B, \pi)$ and O , the observation sequence, find the optimal state sequence for the Markov process.
- (3) Given O , the number of unique symbols M and the number of states N , find λ .

Problem 1 involves determining the likelihood of an observation sequence using the model. Problem 2 deals with uncovering the “hidden” part of the HMM. Problem 3 deals with training the HMM using the given observation sequence O and the parameters M and N .

In this paper we will be dealing with problem 1 and 3. We will make use of methods to solve problem 3 to train a HMM using opcode sequences extracted from executable files. Scoring opcode sequences to be tested using this model involves solving problem 1. We will not be dealing with problem 2, as previous research indicates that the meaning of the HMM states themselves has not been of much consequence to the detection capability of the HMM [12, 30].

5.2.1 Forward Algorithm

The forward algorithm or α pass is used to determine $P(O|\lambda)$.

For $t = 0, 1, \dots, T - 1$ and $i = 0, 1, \dots, N - 1$, define

$$\alpha_t(i) = P(O_0, O_1, \dots, O_t, x_t = q_i | \lambda)$$

The probability of the partial observation sequence up to time t is $\alpha_t(i)$.

Using the forward algorithm, $P(O|\lambda)$ can be computed as shown below:

(1) Let $\alpha_0(i) = \pi_i b_i(O_0)$, for $i = 0, 1, \dots, N - 1$.

(2) For $t = 1, 2, \dots, T - 1$, and $i = 0, 1, \dots, N - 1$, compute

$$\alpha_t(i) = \left[\sum_{j=0}^{N-1} \alpha_{t-1}(j) a_{ji} \right] b_i(O_t).$$

$$(3) P(O|\lambda) = \sum_{i=0}^{N-1} \alpha_{T-1}(i).$$

5.2.2 Backward Algorithm

Backward algorithm or β pass can be used to determine the most likely state sequence.

For $t = 0, 1, \dots, T - 1$ and $i = 0, 1, \dots, N - 1$, define

$$\beta_t(i) = P(O_{t+1}, O_{t+2}, \dots, O_{T-1} | x_t = q_i, \lambda)$$

Then, $\beta_t(i)$ can be computed efficiently as shown below:

(1) Let $\beta_{T-1}(i) = 1$, for $i = 0, 1, \dots, N - 1$.

(2) For $t = T - 2, T - 3, \dots, 0$, and $i = 0, 1, \dots, N - 1$, compute

$$\beta_t(i) = \sum_{j=0}^{N-1} a_{ij} b_j(O_{t+1}) \beta_{t+1}(j).$$

For $t = 0, 1, \dots, T - 2$ and $i = 0, 1, \dots, N - 1$, define

$$\gamma_t(i) = P(x_t = q_i | O, \lambda).$$

Since the relevant probability up to time t is measured by $\alpha_t(i)$, and the relevant probability after time t is measured by $\beta_t(i)$,

$$\gamma_t(i) = \frac{\alpha_t(i) \beta_t(i)}{P(O|\lambda)}.$$

From the definition of $\gamma_t(i)$, the most likely state at any time t is the state for which $\gamma_t(i)$ is maximum.

5.2.3 Baum-Welch Algorithm

This algorithm adjusts model parameters to best-fit the observations. The number of states N and the number of unique observations symbols M are fixed. However, the contents of the A , B and π are free, subject only to the row stochastic condition. The re-estimation process is explained below:

- (1) Initialize $\lambda = (A, B, \pi)$ with an approximate guess. If no such guess is possible, use random values. For example $\pi_i = 1/N$, $A_{ij} = 1/N$, $B_{ij} = 1/M$.
- (2) Compute $\alpha_t(i)$, $\beta_t(i)$, $\gamma_t(i)$ and $\gamma_t(i, j)$ where $\gamma_t(i, j)$ is a di-gamma.

Di-gammas can be defined as:

$$\gamma_t(i) = \frac{\alpha_t(i)a_{ij}b_j(O_{t+1})\beta_{t+1}(j)}{P(O|\lambda)}$$

The $\gamma_t(i)$ and $\gamma_t(i, j)$ (or di-gamma) are related by

$$\gamma_t(i) = \sum_{j=0}^{N-1} \gamma_t(i, j)$$

- (3) Re-estimate model parameters as follows: For $i = 0, 1, \dots, N - 1$ let

$$\pi_i = \gamma_0(i)$$

For $i = 0, 1, \dots, N - 1$ and $j = 0, 1, \dots, N - 1$, compute

$$a_{ij} = \sum_{t=0}^{T-2} \gamma_t(i, j) \Bigg/ \sum_{t=0}^{T-2} \gamma_t(i)$$

For $j = 0, 1, \dots, N - 1$ and $k = 0, 1, \dots, M - 1$, compute

$$b_j(k) = \sum_{t \in \{0, 1, \dots, T-2\}, O_t=k} \gamma_t(j) \Bigg/ \sum_{t=0}^{T-2} \gamma_t(j)$$

- (4) If $P(O|\lambda)$ increases, go to step 3.

5.3 HMMs and Virus detection

The use of HMMs for metamorphic virus detection is explained in great detail in [29, 30]. The basic objective is to train an HMM using opcodes extracted from viruses belonging to a particular family. The trained HMM will, in effect, represent the statistical properties of the virus family. Using this trained HMM, we can compute a score for any given program to determine how “close” the file is to the virus family that the HMM represents. We can then classify the file based on a predetermined threshold.

First, a collection of viruses belonging to the same family are disassembled. From each of the disassembled files, only the instruction opcodes are extracted. An example of extracted opcodes is shown in Figure 5.2. Opcodes sequences extracted from all the virus files are concatenated. This concatenated sequence forms the sequence observations used to train an HMM. The set of unique opcodes in the observation sequence is the set of distinct observation symbols.

An HMM is now trained using this sequence of observations, as explained in Section 5.1.1. To detect whether a given program belongs to the virus family, this trained HMM is used to calculate the Log Likelihood per Opcode (LLPO). If the LLPO of the program is within a particular threshold, the file is classified as belonging to the virus family. We now take a briefly look at what Log Likelihood Per Opcode means.

5.3.1 Log Likelihood Per Opcode

Scoring observation sequences and training the HMM involves computation of product of probabilities. The result of multiplication tends to 0 exponentially as T increases. As a result, the use of methods described in Section 5.2 inevitably results

```

call
mov
mov
mov
xor
call
mov
mov
mov
xor
call
mov
call
mov
call
mov
mov
mov
xor
call
mov
mov
mov
xor
call
xor
call
nop

```

Figure 5.2: Extracted opcode sequence

in underflow. To avoid this problem, the forward and backward algorithms normalize the result of each iteration. This process is called scaling. HMM scaling is explained in detail in [21].

Once scaling is employed, $P(O|\lambda)$ is redefined as:

$$P(O|\lambda) = 1 / \prod_{j=0}^{T-1} c_j$$

where c_j is the scaling factor at time j . However, this computation is also susceptible to underflow and to avoid that, we compute:

$$\log[P(O|\lambda)] = - \sum_{j=0}^{T-1} \log c_j$$

This is the log likelihood. Log likelihood is length dependent, as the sum of log transition probabilities and log observation probabilities will be higher for a

longer sequence. As the sequences in the test set may be of different lengths compared to the sequences used to train the model, log likelihood is divided by the number of opcodes in the sequence to obtain Log Likelihood Per Opcode which accounts for the length difference [30].

5.3.2 Effectiveness of HMM detection

HMM detection has proven to be very effective in detection of highly metamorphic viruses [30]. Experiments with HMM detection in [29] indicate a detection rate of about 90% and a false positive rate of less than 10%.

5.4 Evading HMM detection

There has been some research on methods to evade HMM detection [12]. The method presented in [12] involves inserting dead code from the benign files in the test set, into the virus files. This helps in making the virus files statistically similar to normal files. This is achieved by making use of a dynamic scoring algorithm which inserts a block of dead code only if it results in the virus file becoming more similar [14] to normal files.

Results presented in [11] indicate that, with an increase in the amount of dead code inserted from normal files, the average LLPO scores for viruses and normal files become closer. The HMM-detector showed indications of failing when 5% of the subroutines were copied from the normal file. The LLPO scores for viruses and normal files were the closest when 35% dead blocks and 30% subroutines were copied from normal files.

Results in [11] also indicate that inserting long sequences of opcodes, like subroutines, are more effective in defeating HMM detection than randomly inserted

blocks of dead code. The worm presented in this paper makes use of this result while inserting dead code.

CHAPTER 6

Design and implementation

We have implemented a metamorphic worm that carries its own morphing engine. As mentioned above, this presents a significant challenge since both the worm body and the morphing engine itself must be morphed. This section presents the structure of our metamorphic worm in detail.

6.1 Structure

Figure 6.1 illustrates the structure of the various components of the worm. The worm consists of the following:

- (1) Body - This is the central component that controls the worm's life cycle. It controls and coordinates the activities of all the other active components of the worm.
- (2) Disassembler - Disassembles the binary portion of the worm and extracts instructions from it.
- (3) Morphing Engine - The morphing engine operates on the set of disassembled instructions. It removes old dead code instructions, adds new dead code and employs equivalent instruction substitution.
- (4) Reassembler - The reassembler re-structures the control flow in the morphed body of code and converts the morphed body to binary.
- (5) Payload - This is the actual piece of code the worm is intended to run on every computer it infects. In our case, the payload is benign; it simply

appends a line of text to a temporary file.

- (6) Pad_block_1 and Pad_block_2 (Padding blocks) - These are blocks of dead code that are replaced from generation to generation. The purpose of doing this is to make the worm statistically similar to normal files and thereby evade HMM detection. The blocks also help to avoid relocating sections and other book-keeping information in the executable from generation to generation [12].



Figure 6.1: Metamorphic worm components

6.2 Memory Layout

We now examine the layout of different components of the worm in the address space of the worm's process. The placement of the worm in memory is illustrated in Figure 6.2.

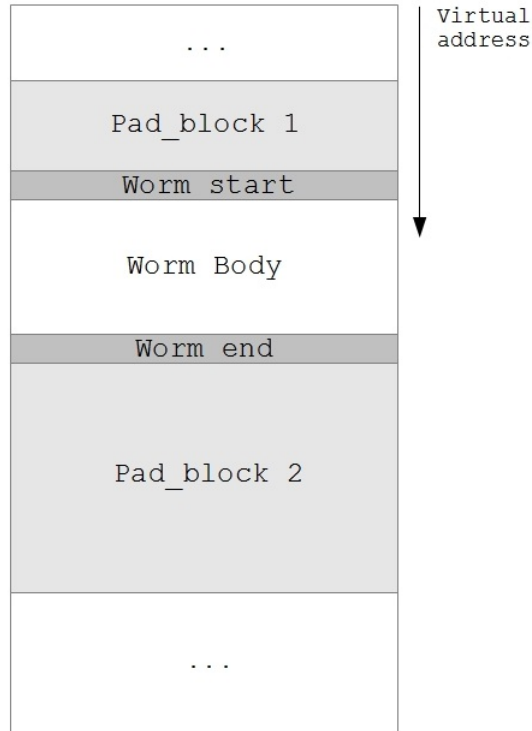


Figure 6.2: Metamorphic worm memory layout

6.3 Metamorphic techniques used

The worm uses two of the metamorphic techniques described in Chapter 3. Specifically, the worm uses equivalent instruction substitution and garbage code insertion.

6.3.1 Equivalent instruction substitution

The primary candidates for morphing are the `MOV` and the `XOR` instructions. The former because, it appears in abundance in binaries, and the latter because it is a usual candidate for substituting the `MOV` instruction and hence needs to be substituted back.

After the disassembler has disassembled the worm-portion of the worm’s executable image, the instructions are scanned for possible equivalent instructions to be substituted, by the morphing engine. These instructions are substituted by equivalent instructions with a fixed probability. This is achieved using a substitution table as shown in Table 6.1.

Table 6.1: Equivalent instruction table

| Instruction | Equivalent | Action |
|-----------------------------|--|-------------------|
| <code>0x48 0x89 0xc3</code> | <code>0x48 0x31 0xdb 0x48 0x01 0xc3</code> | <code>NULL</code> |
| <code>0x48 0x89 0xc1</code> | <code>0x48 0x31 0xc9 0x48 0x01 0xc1</code> | <code>NULL</code> |
| ... | | |

The first column of each of the first two rows in Table 6.1 correspond to instructions `MOV %RAX,%RBX` and `MOV %RAX,%RCX` respectively. The second column of the first two rows correspond to instructions `XOR %RBX,%RBX;` `ADD %RAX,%RBX` and `XOR %RBX,%RCX;` `ADD %RAX,%RCX` respectively. The “Action” field in table is the address of a label inside the morphing function which performs actions specific to the instructions that were substituted. It is `NULL` if no specific action is necessary.

A complete list of equivalent instructions that are substituted by the morphing engine is in Appendix A.

6.3.2 Dead code insertion

Dead instruction insertion involves inserting instructions which do not result in any change in data, or the contents of general purpose registers. The sole purpose of adding these instructions is to increase the diversity of instructions.

However, the effect of such instructions on the RFLAGS register should be carefully considered as they might have adverse effects on control flow. Control flow instructions use bits in the RFLAGS register to decide which code path to take. If a dead code instruction which manipulates RFLAGS is inserted before a control flow instruction, it can have an adverse effect on the result of executing the next control flow instruction.

Examples for dead code instructions include ADD \$0x0,%RAX, SUB \$0x0,%RBX, XOR \$0x0,%RAX, etc. The complete list of dead code instructions used by the worm is in Appendix B.

6.4 Functionality

A characteristic feature of metamorphic malware which carry their own engine is that the actual “payload” part of the worm will be much smaller than the overall size of the worm. In the case of our worm, the payload is benign and merely appends some text to the end of a temporary file. The worm’s functionality is summarized by the Algorithm below:

```
Run ‘‘payload’’ // Actual intent of the worm
```

```
Open own binary image from disk by reading /proc/self/exe
```

```
Read worm data and book-keeping data from its ‘‘.data’’ section
```

Disassemble worm body excluding padding blocks:

For each disassembled instruction:

Add a unique label and store virtual address

Build symbol table:

For each disassembled instruction INS:

if control flow instruction

add (INS.label, INS.target.label) to symbol table

Morph:

Initialize substitution and dead code instruction tables

For each disassembled instruction INS:

if INS is a dead instruction:

if INS is a control flow target

(determined from symbol table)

Change target to the next disassembled instruction

Ignore dead instruction

// Probability to insert dead code instruction = 0.33

if adding new dead code instruction:

choose dead code instruction randomly from table

add new dead code instruction to morphed

instruction list

// Probability to morph an existing instruction

```
// if possible, is 0.33

If morphing:

    Check substitution table for a suitable entry

        if valid entry exists:

            Add instructions to be substituted to

            morphed instructions list

    Recalculate virtual addresses
```

Reassembly:

```
Fix control flow in list of morphed instructions
```

Patch new binary:

```
Replace padding blocks from benign binaries

Create a new binary image

Write binary to disk
```

Propogate:

```
// This is for completeness only. A real worm uses exploits
‘‘rcp’’ or ‘‘scp’’ the new binary image to surrounding IP
addresses
```

6.5 Implementation

The worm is implemented to work on Linux on the Intel x86_64 architecture. The programming language used to implement the worm is C. The compiler used to build the worm is GCC, version 4.6.2 build 20111027 and the resulting format of the

executable image of the worm is ELF64. This section explains implementation details such as layout of the worm’s executable image, libraries used by the worm, etc.

6.5.1 Libraries used

The worm only links directly to libc and libdl. The libraries dynamically loaded during run-time are libbfd and libopdis. Libraries libc and libdl are part of the core of any Linux distribution. Libbfd is part of the GNU Binutils [13] package, and is usually found on most of the Linux distributions. Libopdis is an independent library licensed under GNU LGPL as of version 1.0.4 [16]. Libopdis extends the libopcodes library [13] by offering algorithms for linear and control-flow disassembly, instruction and operand objects that are suitable for analysis.

CHAPTER 7

Experiments

The effectiveness of the worm is evaluated using n-gram similarity [14], similarity using graph technique [18] and HMM based detection [30].

For the worm to be effective in evading signature based detection, the worm bodies in different generations of worm files must not be too similar to one another. At the same time, the worm files must be similar to benign files so that they are not easily distinguishable from benign files based on a similarity threshold [18].

An effective means of evading HMM based detection is to make the worms statistically similar to benign binaries. This achieved by using long sequences of instructions from benign executable files to fill the worm's padding blocks. This is in line with the HMM evasion technique [12] discussed in Section 5.4.

7.1 Test data

For each experiment, 100 generations of the worm are generated and 20 benign files are selected. The list of benign files, and their corresponding file IDs used in our test cases are shown in Table 7.1. From the 100 worms, 80 worms are chosen to train the HMM. The remaining 20 worms and benign files are scored using the trained HMM. The worm files in the test set are named MWOR_0, MWOR_1, ..., MWOR_19. The benign files are named BEN_0, BEN_1, ..., BEN_19.

The padding blocks of the MWOR files are randomly chosen blocks of code from one or more of the BEN files. Replacing the padding block randomly from the chosen benign file set in Table 7.1 is part of the worm's functionality.

Table 7.1: Mapping from Benign file ID to actual executable file

| Benign file ID | Actual executable file |
|----------------|------------------------|
| BEN_0 | /usr/bin/as |
| BEN_1 | /usr/bin/date |
| BEN_2 | /usr/bin/dmesg |
| BEN_3 | /usr/bin/file |
| BEN_4 | /usr/bin/gcc |
| BEN_5 | /usr/bin/size |
| BEN_6 | /usr/bin/grep |
| BEN_7 | /usr/bin/kill |
| BEN_8 | /usr/bin/ld |
| BEN_9 | /usr/bin/ldd |
| BEN_10 | /usr/bin/mknod |
| BEN_11 | /usr/bin/mount |
| BEN_12 | /usr/bin/nasm |
| BEN_13 | /usr/bin/nm |
| BEN_14 | /usr/bin/objdump |
| BEN_14 | /usr/bin/readelf |
| BEN_15 | /usr/bin/rm |
| BEN_16 | /usr/bin/sleep |
| BEN_17 | /usr/bin/strip |
| BEN_18 | /usr/bin/systemctl |
| BEN_19 | /usr/bin/touch |

As part of the experiment, both n-gram and graph technique are used to measure similarity between worms, between worms and benign files, and between benign files. An HMM classifier trained using worm files in the training set, is used to score benign files and worm files in the test set.

7.2 N-gram Similarity

The n-gram similarity technique [14] explained in Section 4.1 is used to measure similarity between opcode sequences extracted from different generations of the worm and from benign executable files. Since the objective here is to assess whether common signatures can be extracted from worm executable files, the

padding blocks are excluded from the assessment. When comparing these worm bodies to benign files, a representative sample sequence of instructions, of length equal to that of the worm body is chosen from the benign files.

Table 7.2 lists the similarity scores between consecutive generations of the worm. The average similarity is 19.09%. Similarly, Table 7.3 and Table 7.4 list the similarity scores between worms and benign files, and between worm files respectively. The average similarity between worms and benign files is 13.98%, while the average similarity between benign files is 26.35%.

Table 7.2: Similarity between MWOR files

| File 1 | File 2 | Similarity | File 1 | File 2 | Similarity |
|--------------------|---------|------------|---------|---------|------------|
| MWOR_0 | MWOR_1 | 0.209329 | MWOR_10 | MWOR_11 | 0.167043 |
| MWOR_1 | MWOR_2 | 0.139122 | MWOR_11 | MWOR_12 | 0.220303 |
| MWOR_2 | MWOR_3 | 0.199484 | MWOR_12 | MWOR_13 | 0.170271 |
| MWOR_3 | MWOR_4 | 0.21417 | MWOR_13 | MWOR_14 | 0.142834 |
| MWOR_4 | MWOR_5 | 0.222563 | MWOR_14 | MWOR_15 | 0.133796 |
| MWOR_5 | MWOR_6 | 0.526146 | MWOR_15 | MWOR_16 | 0.179309 |
| MWOR_6 | MWOR_7 | 0.206423 | MWOR_16 | MWOR_17 | 0.120562 |
| MWOR_7 | MWOR_8 | 0.225307 | MWOR_17 | MWOR_18 | 0.133473 |
| MWOR_8 | MWOR_9 | 0.133635 | MWOR_18 | MWOR_19 | 0.126372 |
| MWOR_9 | MWOR_10 | 0.15623 | | | |
| Mean: 0.190862 | | | | | |
| Variance: 0.007521 | | | | | |

The similarity between worm generations can also be visualized graphically as explained in Section 4. The similarity between the first and second generations of the worm is illustrated by the graph in Figure 7.1. Examples of the other graphs depicting the similarity between other consecutive pairs of worms are included in Appendix C.

The n-gram similarity between worms, is somewhat lower than the similarity between benign files. This can be attributed to the fact that, only the worm body is

Table 7.3: Similarity between MWOR and benign files

| File 1 | File 2 | Similarity | File 1 | File 2 | Similarity |
|--------------------|--------|------------|---------|--------|------------|
| MWOR_0 | BEN_0 | 0.203112 | MWOR_10 | BEN_10 | 0.234278 |
| MWOR_1 | BEN_1 | 0.118454 | MWOR_11 | BEN_11 | 0.130494 |
| MWOR_2 | BEN_2 | 0.178677 | MWOR_12 | BEN_12 | 0.125905 |
| MWOR_3 | BEN_3 | 0.105231 | MWOR_13 | BEN_13 | 0.141814 |
| MWOR_4 | BEN_4 | 0.17498 | MWOR_14 | BEN_14 | 0.068771 |
| MWOR_5 | BEN_5 | 0.121704 | MWOR_15 | BEN_15 | 0.050677 |
| MWOR_6 | BEN_6 | 0.133385 | MWOR_16 | BEN_16 | 0.123899 |
| MWOR_7 | BEN_7 | 0.169622 | MWOR_17 | BEN_17 | 0.118309 |
| MWOR_8 | BEN_8 | 0.152165 | MWOR_18 | BEN_18 | 0.181743 |
| MWOR_9 | BEN_9 | 0.13086 | MWOR_19 | BEN_19 | 0.131365 |
| Mean: 0.139772 | | | | | |
| Variance: 0.001732 | | | | | |

Table 7.4: Similarity between BEN files

| File 1 | File 2 | Similarity | File 1 | File 2 | Similarity |
|--------------------|--------|------------|--------|--------|------------|
| BEN_0 | BEN_1 | 0.223816 | BEN_10 | BEN_11 | 0.212141 |
| BEN_1 | BEN_2 | 0.176202 | BEN_11 | BEN_12 | 0.213142 |
| BEN_2 | BEN_3 | 0.309048 | BEN_12 | BEN_13 | 0.399767 |
| BEN_3 | BEN_4 | 0.248399 | BEN_13 | BEN_14 | 0.249333 |
| BEN_4 | BEN_5 | 0.196715 | BEN_14 | BEN_15 | 0.190627 |
| BEN_5 | BEN_6 | 0.227521 | BEN_15 | BEN_16 | 0.450179 |
| BEN_6 | BEN_7 | 0.199912 | BEN_16 | BEN_17 | 0.215491 |
| BEN_7 | BEN_8 | 0.240475 | BEN_17 | BEN_18 | 0.412275 |
| BEN_8 | BEN_9 | 0.248165 | BEN_18 | BEN_19 | 0.327552 |
| BEN_9 | BEN_10 | 0.265344 | | | |
| Mean: 0.263479 | | | | | |
| Variance: 0.006037 | | | | | |

considered for similarity tests, rather than the whole worm. The same is true in the case of worms versus benign files. The initial sections of the benign files, which are not morphed, result in a higher similarity between benign files, as opposed to worm versus benign files. However, low similarity of the worm body between different generations of the worm, helps evade signature based detection.

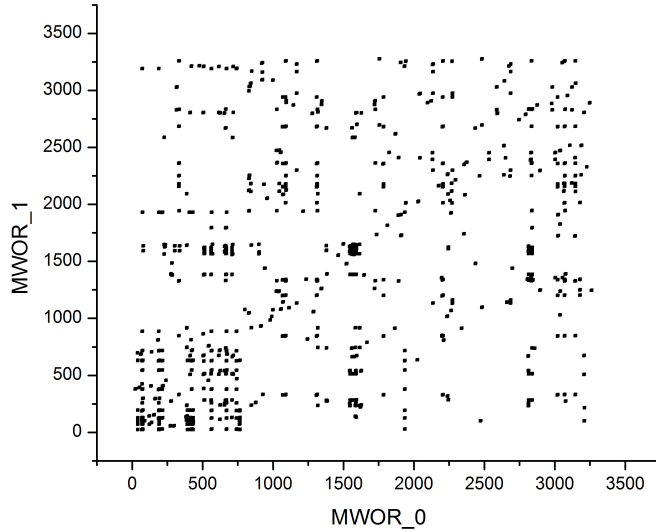


Figure 7.1: Similarity graph MWOR_0 vs MWOR_1

7.3 Similarity using graph technique

The graph technique to measure similarity [18] explained in Section 4.2 is used to measure similarity between complete worm executable files, including padding blocks. It is also used to compare the similarities between pairs benign files, and pairs of worm files and benign files.

Figure 7.2 illustrates the similarity between worm files, benign files, and worm and benign file pairs. The average similarity score for pairs of worm files is 0.592744. The average similarity score for pairs of worms and benign files is 0.565945. The average similarity score for pairs of benign files is 0.667563. As indicated by the similarity scores in Figure 7.2, it is clear that it is not possible to obtain a threshold that can be used to distinguish between the worm files and benign files.

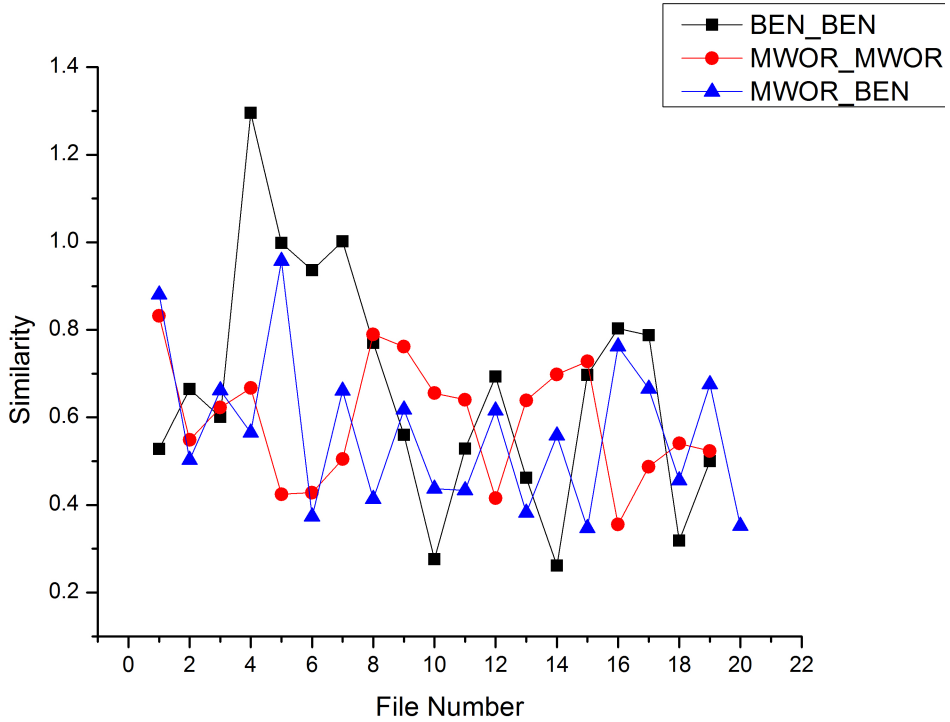


Figure 7.2: Similarity using graph technique

Table 7.5 lists the similarity scores between consecutive generations of the worm. Similarly, Table 7.6 and Table 7.7 list the similarity scores between worms and benign files, and between worm files respectively.

7.4 HMM

We now analyze the results of running the HMM detector on test data. As indicated by previous research [12, 30], the number of states in the HMM does not significantly impact the accuracy of classifier. Consequently, in this chapter, we will only consider HMMs with two hidden states. Additional results for HMMs with three states are presented in Appendix D.

The ratio of dead-code to worm-code, called the “padding-ratio”, is the ratio

Table 7.5: Similarity using graph technique - MWOR files

| File 1 | File 2 | Similarity | File 1 | File 2 | Similarity |
|--------------------|---------|------------|---------|---------|------------|
| MWOR_0 | MWOR_1 | 0.831699 | MWOR_10 | MWOR_11 | 0.64038 |
| MWOR_1 | MWOR_2 | 0.548553 | MWOR_11 | MWOR_12 | 0.41586 |
| MWOR_2 | MWOR_3 | 0.622553 | MWOR_12 | MWOR_13 | 0.638838 |
| MWOR_3 | MWOR_4 | 0.667299 | MWOR_13 | MWOR_14 | 0.698381 |
| MWOR_4 | MWOR_5 | 0.424688 | MWOR_14 | MWOR_15 | 0.727753 |
| MWOR_5 | MWOR_6 | 0.428372 | MWOR_15 | MWOR_16 | 0.355481 |
| MWOR_6 | MWOR_7 | 0.504638 | MWOR_16 | MWOR_17 | 0.487425 |
| MWOR_7 | MWOR_8 | 0.78983 | MWOR_17 | MWOR_18 | 0.540405 |
| MWOR_8 | MWOR_9 | 0.761414 | MWOR_18 | MWOR_19 | 0.523221 |
| MWOR_9 | MWOR_10 | 0.655345 | | | |
| Mean: 0.592744 | | | | | |
| Variance: 0.017882 | | | | | |

Table 7.6: Similarity using graph technique - MWOR and BEN files

| File 1 | File 2 | Similarity | File 1 | File 2 | Similarity |
|--------------------|--------|------------|---------|--------|------------|
| MWOR_0 | BEN_0 | 0.880288 | MWOR_10 | BEN_10 | 0.433276 |
| MWOR_1 | BEN_1 | 0.502868 | MWOR_11 | BEN_11 | 0.615871 |
| MWOR_2 | BEN_2 | 0.661706 | MWOR_12 | BEN_12 | 0.381922 |
| MWOR_3 | BEN_3 | 0.565231 | MWOR_13 | BEN_13 | 0.558548 |
| MWOR_4 | BEN_4 | 0.957393 | MWOR_14 | BEN_14 | 0.34732 |
| MWOR_5 | BEN_5 | 0.373347 | MWOR_15 | BEN_15 | 0.761746 |
| MWOR_6 | BEN_6 | 0.660952 | MWOR_16 | BEN_16 | 0.665618 |
| MWOR_7 | BEN_7 | 0.413928 | MWOR_17 | BEN_17 | 0.455879 |
| MWOR_8 | BEN_8 | 0.618177 | MWOR_18 | BEN_18 | 0.675529 |
| MWOR_9 | BEN_9 | 0.437322 | MWOR_19 | BEN_19 | 0.35198 |
| Mean: 0.565945 | | | | | |
| Variance: 0.028684 | | | | | |

of number of dead code instructions in the worm to the number of instructions that correspond to the worm's functionality. For example, a worm with twice as much dead code as worm instructions will have a padding-ratio of 2.

We use an HMM with two states to score worms with padding ratio: 0.5, 1, 1.5, 2, 2.5, 3 and 4. Using these scores, we analyze the padding-ratio for which the HMM detector starts to falter.

Table 7.7: Similarity using graph technique - BEN files

| File 1 | File 2 | Similarity | File 1 | File 2 | Similarity |
|--------------------|--------|------------|--------|--------|------------|
| BEN_0 | BEN_1 | 0.527698 | BEN_10 | BEN_11 | 0.528616 |
| BEN_1 | BEN_2 | 0.665027 | BEN_11 | BEN_12 | 0.693015 |
| BEN_2 | BEN_3 | 0.601069 | BEN_12 | BEN_13 | 0.462323 |
| BEN_3 | BEN_4 | 1.295305 | BEN_13 | BEN_14 | 0.261346 |
| BEN_4 | BEN_5 | 0.998744 | BEN_14 | BEN_15 | 0.696717 |
| BEN_5 | BEN_6 | 0.936357 | BEN_15 | BEN_16 | 0.802703 |
| BEN_6 | BEN_7 | 1.00245 | BEN_16 | BEN_17 | 0.787582 |
| BEN_7 | BEN_8 | 0.770225 | BEN_17 | BEN_18 | 0.318344 |
| BEN_8 | BEN_9 | 0.559742 | BEN_18 | BEN_19 | 0.500018 |
| BEN_9 | BEN_10 | 0.276418 | | | |
| Mean: 0.667563 | | | | | |
| Variance: 0.068312 | | | | | |

Figure 7.3 shows the result of scoring worms and benign files that are part of the test data, using an HMM with two states. In this case, the generated worms contain half as much dead code as the instructions that constitute the core functionality of the worm.

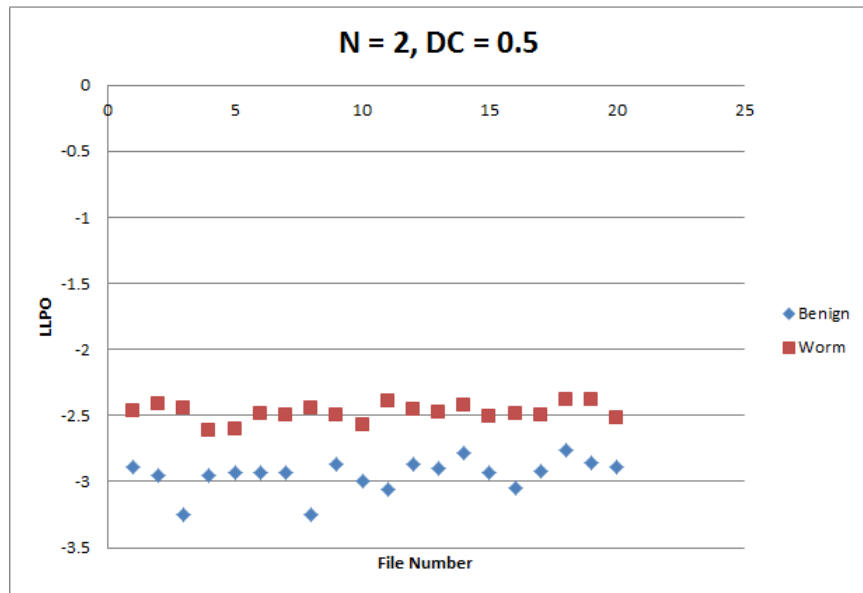


Figure 7.3: HMM with $N = 2$, padding-ratio: 0.5

The Log Likelihood Per Opcode (LLPO) scores for each of the MWOR files and BEN files are shown in Table 7.8.

Table 7.8: LLPO scores - padding-ratio: 0.5, N=2

| File | LLPO | File | LLPO |
|--------|-----------|---------|-----------|
| BEN_0 | -2.887989 | MWOR_0 | -2.462167 |
| BEN_1 | -2.953637 | MWOR_1 | -2.409931 |
| BEN_2 | -3.254619 | MWOR_2 | -2.447955 |
| BEN_3 | -2.955244 | MWOR_3 | -2.614725 |
| BEN_4 | -2.933179 | MWOR_4 | -2.604744 |
| BEN_5 | -2.93336 | MWOR_5 | -2.488717 |
| BEN_6 | -2.930817 | MWOR_6 | -2.491995 |
| BEN_7 | -3.248653 | MWOR_7 | -2.448593 |
| BEN_8 | -2.864609 | MWOR_8 | -2.501309 |
| BEN_9 | -2.993974 | MWOR_9 | -2.575815 |
| BEN_10 | -3.063865 | MWOR_10 | -2.388594 |
| BEN_11 | -2.868419 | MWOR_11 | -2.456711 |
| BEN_12 | -2.898413 | MWOR_12 | -2.471223 |
| BEN_13 | -2.784516 | MWOR_13 | -2.424988 |
| BEN_14 | -2.934695 | MWOR_14 | -2.502634 |
| BEN_15 | -3.044624 | MWOR_15 | -2.488669 |
| BEN_16 | -2.91717 | MWOR_16 | -2.493647 |
| BEN_17 | -2.758506 | MWOR_17 | -2.385327 |
| BEN_18 | -2.859302 | MWOR_18 | -2.381464 |
| BEN_19 | -2.890073 | MWOR_19 | -2.515267 |

Figure 7.4 shows the scores for a padding-ratio of 2.5. The increase in padding-ratio causes the LLPO scores of the worms to be closer to that of benign binaries.

The same test is repeated for other padding ratios. The results of the test are summarized in the ROC curve shown in Figure 7.5. The area under the curve (AUC) is equal to the probability that a classifier will rank a randomly chosen positive instance higher than a randomly chosen negative one [5].

The AUC and standard error for each of the curves in the graph is shown in

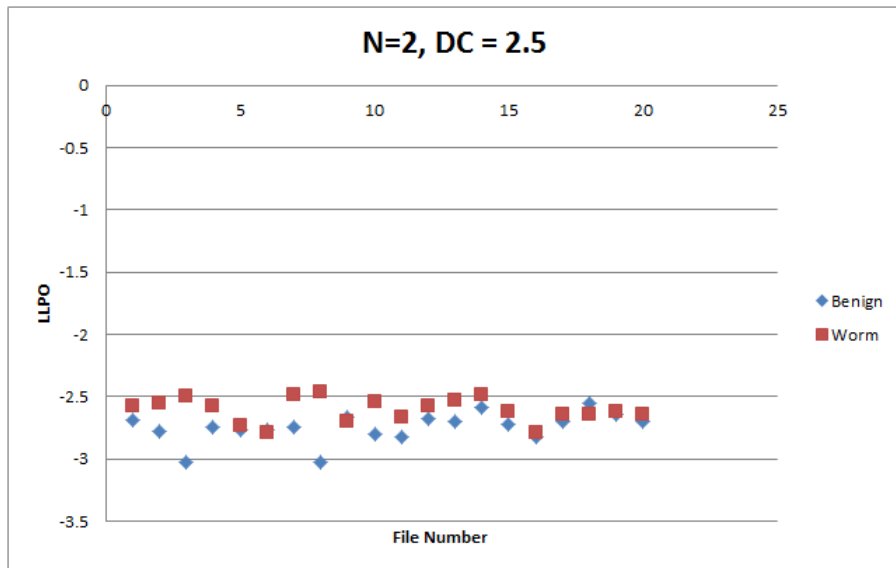


Figure 7.4: HMM with $N = 2$, padding-ratio 2.5

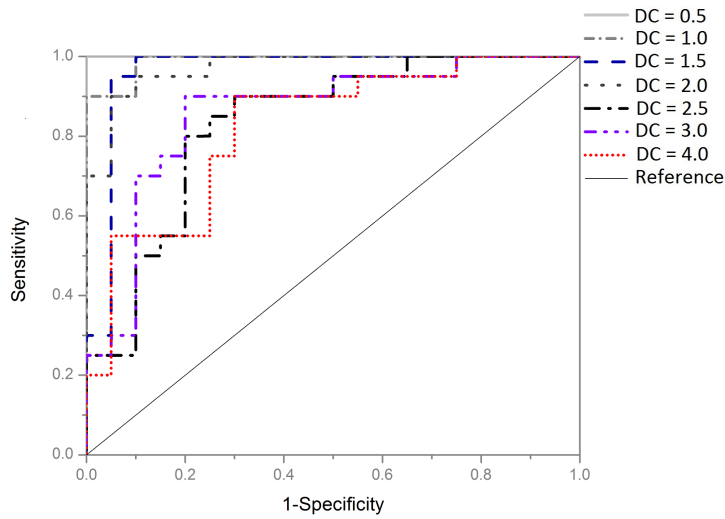


Figure 7.5: ROC Curves for different padding-ratios

Table 7.9. For a padding-ratio of 2.5, the area under the curve is 0.8325. At this point the it is safe to assume the HMM detector starts misclassifying files with some probability.

Table 7.9: ROC AUC statistics for different padding-ratios

| Padding-ratio | AUC | Standard Error |
|---------------|--------|----------------|
| 0.5 | 1 | 0 |
| 1.0 | 0.99 | 0.0105 |
| 1.5 | 0.9625 | 0.03503 |
| 2.0 | 0.9725 | 0.02112 |
| 2.5 | 0.8325 | 0.06556 |
| 3.0 | 0.8575 | 0.06225 |
| 4.0 | 0.8225 | 0.06661 |

CHAPTER 8

Conclusion

The metamorphic worm described in this paper makes use of two morphing techniques: equivalent instruction substitution and dead instruction insertion. This is done in order to defeat signature-based detection. The worm also uses blocks of dead code from benign executable files to evade HMM detection. This also helps in making the worm executable files similar to benign executable files.

Results from the experiments show that it is not possible to obtain useful detection results using an HMM-based detector when the added dead code is more than 2.5 times the worm code. The HMM detector's performance is acceptable for padding-ratios up to 2.0. However, the probability of misclassification starts increasing for padding-ratios 2.5 and above, as indicated by the ROC curves.

We measured similarity using n-gram technique and graph technique between various combinations of benign executable files and worm files. The n-gram similarity between worm bodies in different generations of the worm, is sufficiently low to avoid extraction of a common signature, which can be used for signature-based detection.

The average similarity scores measured using graph technique, between worm file pairs, and between worm file and benign file pairs, are comparable to the similarity scores of benign file pairs. Therefore, the worms cannot be distinguished from benign files based on a similarity threshold.

CHAPTER 9

Future work

One of the main techniques used by the metamorphic worm described in this paper, is garbage instruction insertion. Use of garbage instructions is a proven technique to defeat the HMM detector [12]. However, the instructions are inserted randomly at feasible places and can be separated using more advanced dead-instruction finding tools. Further research can be done on such tools which can effectively detect functionally equivalent blocks of dead code.

Further research needs to be done on evaluating the effectiveness of HMM-based detectors, when compiler generated blocks of non-functional code are used for morphing.

The worm also uses simple morphing techniques. Further research can be carried out on morphing engines which use more advanced morphing techniques, while retaining the ability to be carried along with the malware.

LIST OF REFERENCES

- [1] S. Attaluri, S. McGhee, and M. Stamp. Profile hidden markov models and metamorphic virus detection. *Journal in Computer Virology*, 5(2):151–169, 2009.
- [2] J. Aycock. *Computer Viruses and Malware (Advances in Information Security)*. Springer-Verlag New York, Inc., Secaucus, NJ, USA, 2006.
- [3] P. Beaucamps. Advanced Metamorphic Techniques in Computer Viruses. In *International Conference on Computer, Electrical, and Systems Science, and Engineering - CESSE'07*, Venice, Italy, 2007.
- [4] V. Bontchev. Possible virus attacks against integrity programs and how to prevent them. In *In Virus Bulletin Conference*, pages 131–141, 1992.
- [5] A. P. Bradley. The use of the area under the roc curve in the evaluation of machine learning algorithms. *Pattern Recognition*, 30:1145–1159, 1997.
- [6] P. Desai. Towards an undetectable computer virus (2008). *Master's Projects. Paper 90*. http://scholarworks.sjsu.edu/etd_projects/90.
- [7] T. M. Driller. Metamorphism in practice or “How I made MetaPHOR and what I’ve learnt”, 2002. <http://vx.netlux.org/lib/vmd01.html>.
- [8] E. Filoli. Metamorphism, formal grammars and undecidable code mutation. *International Journal of Computer Science*, 2:70–75, 2007.
- [9] N. Idika and A. P. Mathur. A survey of malware detection techniques. *Purdue University*, page 48, 2007.
- [10] E. Konstantinou, S. Wolthusen, and R. Holloway. Metamorphic virus: Analysis and detection, 2008.
- [11] D. Lin. Hunting for undetectable metamorphic viruses (2009). *Master's Projects. Paper 18*. http://scholarworks.sjsu.edu/etd_projects/18.
- [12] D. Lin and M. Stamp. Hunting for undetectable metamorphic viruses. *J. Comput. Virol.*, 7(3):201–214, Aug. 2011.
- [13] F. Miller, A. Vandome, and J. McBrewster. *Gnu Binutils*. Alphascript Publishing, 2010.

- [14] P. Mishra. Taxonomy of uniqueness transformations (2003).
<http://www.cs.sjsu.edu/faculty/stamp/students/FinalReport.doc>.
- [15] C. Nachenberg. Computer virus-antivirus coevolution. *Commun. ACM*, 40(1):46–51, Jan. 1997.
- [16] Opdis. libopcodes-based disassembler, 2010. <http://mkfs.github.com/content/opdis/>.
- [17] L. R. Rabiner. A tutorial on hidden markov models and selected applications in speech recognition. In *Proceedings of the IEEE*, pages 257–286, 1989.
- [18] N. Runwal, R. M. Low, and M. Stamp. Opcode graph similarity and metamorphic detection. *Journal in Computer Virology*, 8(1-2):37–52, 2012.
- [19] Snakebyte. Next Generation Virus Construktion Kit (NGVCK), 2000.
<http://vx.netlux.org/vx.php?id=tn02>.
- [20] M. Stamp. *Information Security: Principles and Practice*. John Wiley & Sons, 2011.
- [21] M. Stamp. A revealing introduction to hidden markov models, 2012.
<http://www.cs.sjsu.edu/~stamp/RUA/HMM.pdf>.
- [22] Symantec. What is the difference between viruses, worms, and trojans?, 2006.
<http://service1.symantec.com/support/nav.nsf/docid/1999041209131106>.
- [23] P. Szor. *The Art of Computer Virus Research and Defense*. Addison-Wesley Professional, 2005.
- [24] P. Szor and P. Ferrie. Hunting for metamorphic. In *In Virus Bulletin Conference*, pages 123–144, 2001.
- [25] S. Venkatachalam. Detecting undetectable computer viruses (2010). *Master’s Projects. Paper 156*. http://scholarworks.sjsu.edu/etd_projects/156.
- [26] A. Venkatesan. Code obfuscation and virus detection (2008). *Master’s Projects. Paper 116*. http://scholarworks.sjsu.edu/etd_projects/116.
- [27] G. Wagener, R. State, and A. Dulaunoy. Malware behaviour analysis. *Journal in Computer Virology*, 4(4):279–287, 2008.
- [28] A. Walenstein, R. Mathur, M. R. Chouchane, and A. Lakhotia. The design space of metamorphic malware. In *Proceedings of the 2nd International Conference on Information Warfare*, 2007.

- [29] W. Wong. Analysis and detection of metamorphic computer viruses (2006). *Master's Projects. Paper 153.* http://scholarworks.sjsu.edu/etd_projects/153.
- [30] W. Wong and M. Stamp. Hunting for metamorphic engines. *Journal in Computer Virology*, 2(3):211–229, 2006.
- [31] P. Zbitskiy. Code mutation techniques by means of formal grammars and automata. *Journal in Computer Virology*, 5:199–207, 2009.

APPENDIX A

Equivalent instructions used by the worm

Table A.1: Equivalent instructions used by the worm

| No. | Instruction | Equivalent instruction(s) |
|-----|--------------------|---|
| 1 | MOV IMM, %REG | XOR %REG, %REG ADD IMM, %REG OR XOR %REG, %REG SUB -IMM, %REG |
| 2 | MOV %REG1, %REG2 | XOR %REG2, %REG2 ADD %REG1, %REG2 |
| 3 | MOV %REG1, (%REG2) | MOV \$0, (%REG2) ADD %REG1, (%REG2) |
| 4 | MOV IMM, (%REG) | MOV \$0, (%REG2) ADD IMM, (%REG2) |
| 5 | XOR %REG, %REG | MOV \$0, %REG |

APPENDIX B

Dead code instructions used by the worm

Table B.1: Dead code instructions used by the worm

| No. | Instruction |
|-----|----------------|
| 1 | ADD \$0, %RAX |
| 2 | ADD \$0, %RBX |
| 3 | ADD \$0, %RCX |
| 4 | ADD \$0, %RDX |
| 5 | SUB \$0, %RAX |
| 6 | SUB \$0, %RBX |
| 7 | SUB \$0, %RCX |
| 8 | SUB \$0, %RDX |
| 9 | XOR \$0, %RAX |
| 10 | XOR \$0, %RBX |
| 11 | XOR \$0, %RCX |
| 12 | XOR \$0, %RDX |
| 13 | AND %RAX, %RAX |
| 14 | AND %RBX, %RBX |
| 15 | AND %RCX, %RCX |
| 16 | AND %RDX, %RDX |

APPENDIX C

Similarity Graphs

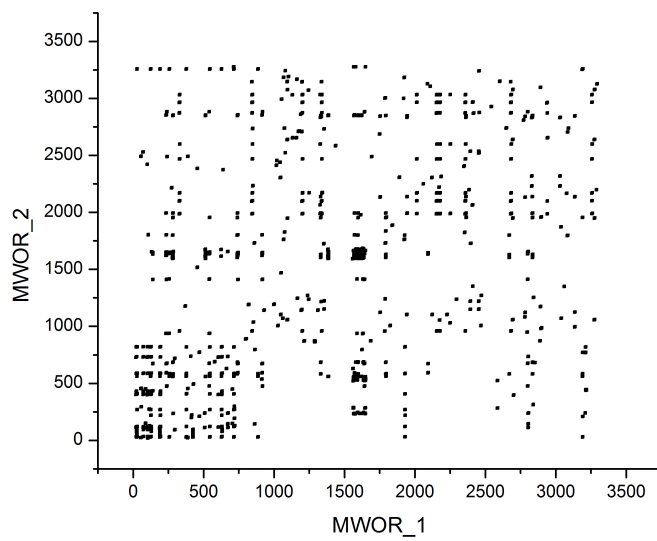


Figure C.1: Similarity graph - MWOR_1 vs MWOR_2

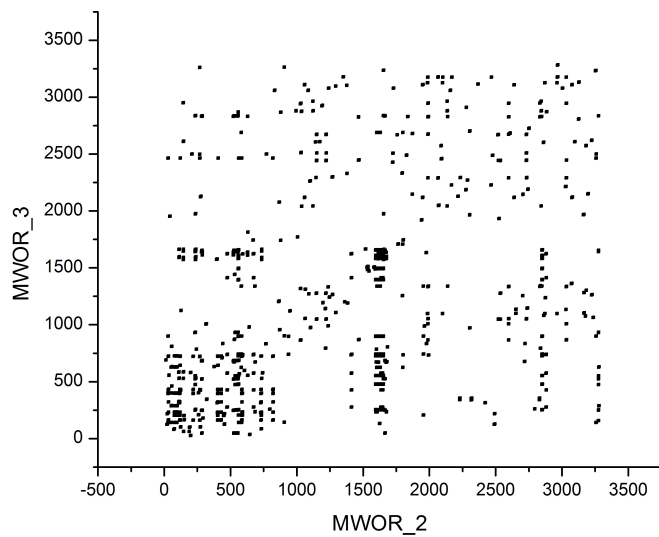


Figure C.2: Similarity graph - MWOR_2 vs MWOR_3

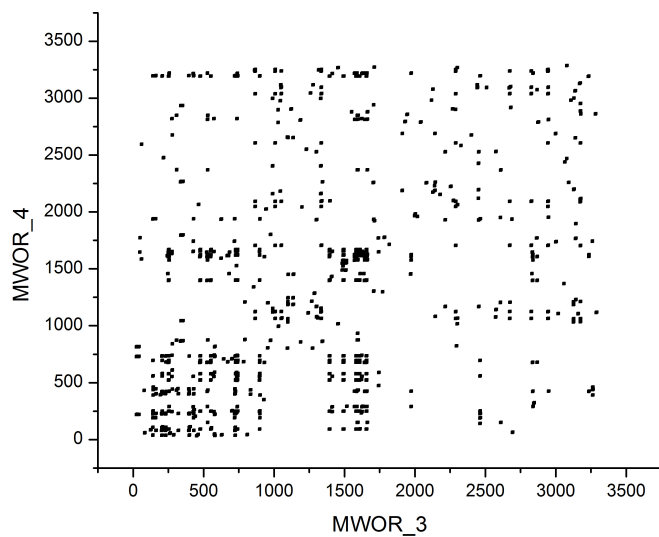


Figure C.3: Similarity graph - MWOR_3 vs MWOR_4

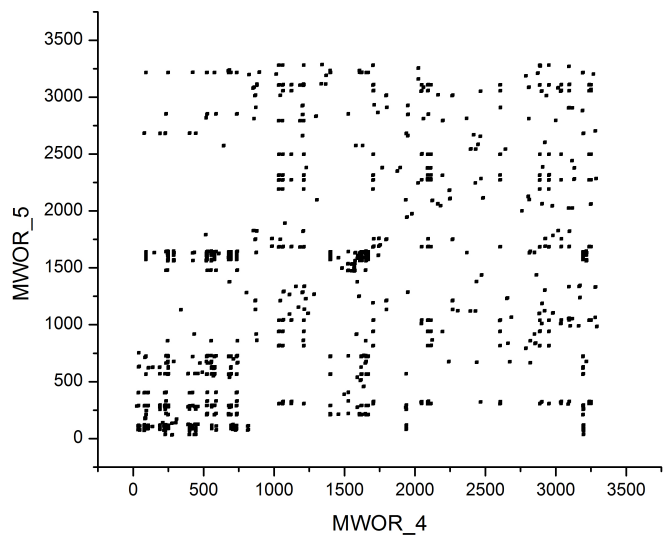


Figure C.4: Similarity graph - MWOR_4 vs MWOR_5

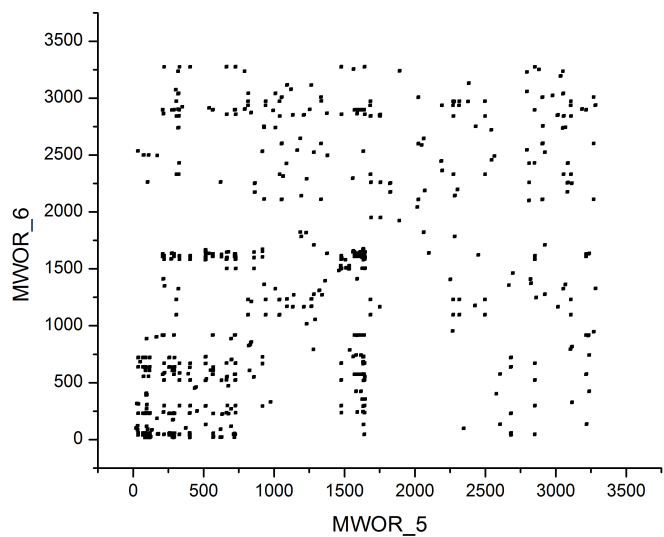


Figure C.5: Similarity graph - MWOR_5 vs MWOR_6

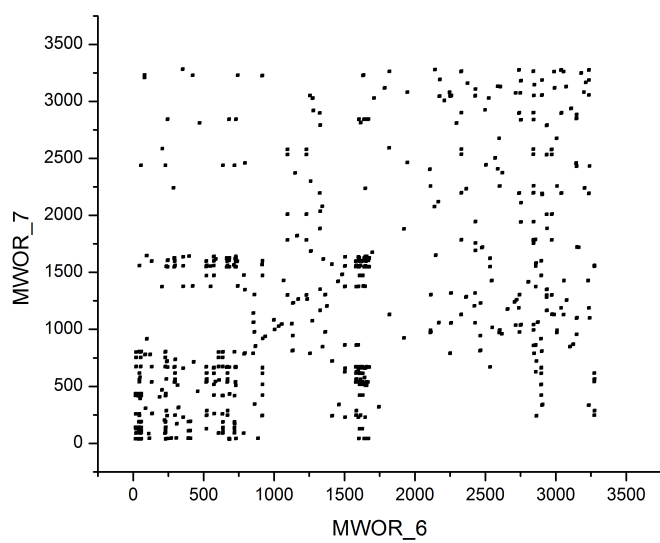


Figure C.6: Similarity graph - MWOR_6 vs MWOR_7

APPENDIX D

Additional HMM results

- HMM parameters: $N = 3, M = 131$
- Worm to padding ratio: 2.0
- LLPO scores: Table D.1
- Lowest MWOR file LLPO: -2.555177
- Highest BEN file LLPO: -2.479824
- Graph: Figure D.1

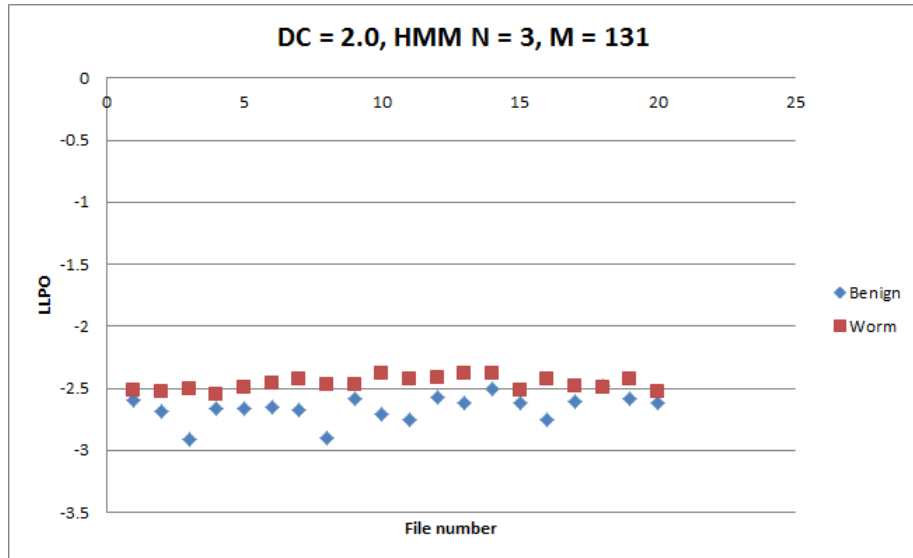


Figure D.1: HMM with $N = 3$, worm-padding ratio 2.0

- (1) HMM parameters: $N = 3, M = 129$

- (2) Worm to padding ratio: 3.0
- (3) LLPO scores: Table D.2
- (4) Lowest MWOR file LLPO: -2.541051
- (5) Highest BEN file LLPO: -2.451643
- (6) Graph: Figure D.2

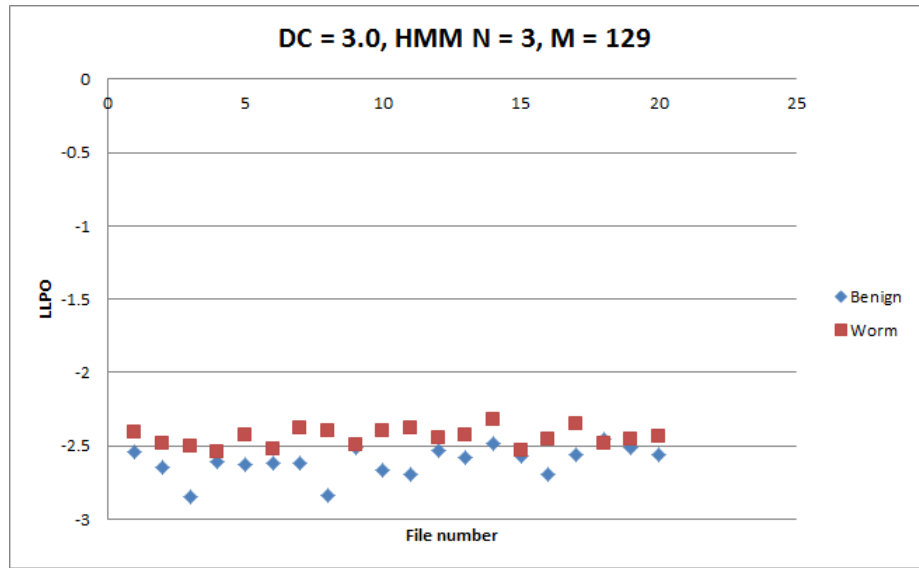


Figure D.2: HMM with $N = 3$, worm-padding ratio 3.0

- (1) HMM parameters: $N = 3$, $M = 131$
- (2) Worm to padding ratio: 4.0
- (3) LLPO scores: Table D.3
- (4) Lowest MWOR file LLPO: -2.718673
- (5) Highest BEN file LLPO: -2.451643
- (6) Graph: Figure D.3

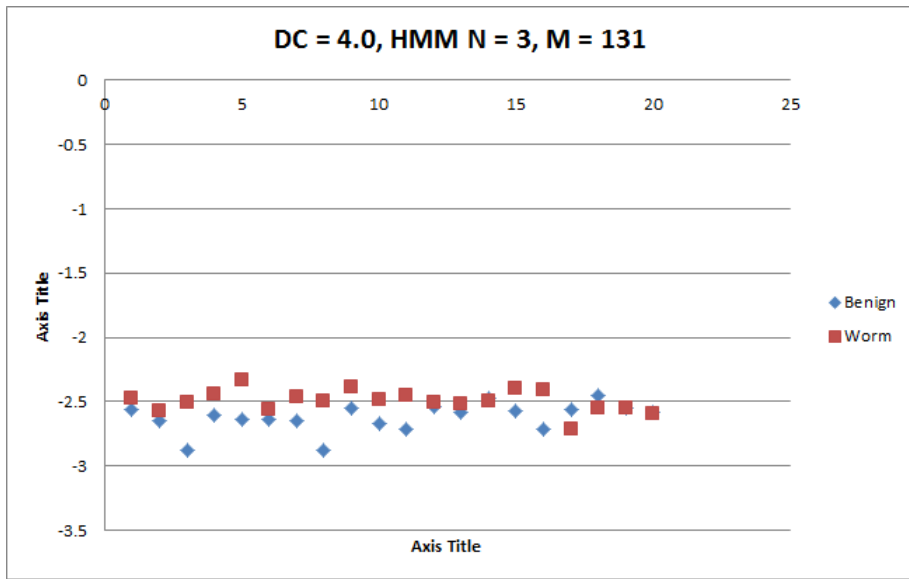


Figure D.3: HMM with $N = 3$, worm-padding ratio 4.0

Table D.1: LLPO scores - Worm-padding ratio: 2.0, $N=3$

| File | LLPO | File | LLPO |
|--------|-----------|---------|-----------|
| File | LLPO | File | LLPO |
| BEN_0 | -2.599386 | MWOR_0 | -2.512852 |
| BEN_1 | -2.684883 | MWOR_1 | -2.529261 |
| BEN_2 | -2.907455 | MWOR_2 | -2.499819 |
| BEN_3 | -2.657581 | MWOR_3 | -2.555177 |
| BEN_4 | -2.661491 | MWOR_4 | -2.492141 |
| BEN_5 | -2.655631 | MWOR_5 | -2.456433 |
| BEN_6 | -2.674456 | MWOR_6 | -2.425267 |
| BEN_7 | -2.900707 | MWOR_7 | -2.470162 |
| BEN_8 | -2.585162 | MWOR_8 | -2.47152 |
| BEN_9 | -2.709333 | MWOR_9 | -2.37629 |
| BEN_10 | -2.756476 | MWOR_10 | -2.427578 |
| BEN_11 | -2.573857 | MWOR_11 | -2.412057 |
| BEN_12 | -2.613086 | MWOR_12 | -2.383274 |
| BEN_13 | -2.508351 | MWOR_13 | -2.381367 |
| BEN_14 | -2.615704 | MWOR_14 | -2.511594 |
| BEN_15 | -2.748886 | MWOR_15 | -2.42333 |
| BEN_16 | -2.603163 | MWOR_16 | -2.477987 |
| BEN_17 | -2.479824 | MWOR_17 | -2.49241 |
| BEN_18 | -2.579598 | MWOR_18 | -2.427912 |
| BEN_19 | -2.613378 | MWOR_19 | -2.533057 |

Table D.2: LLPO scores - Worm-padding ratio: 3.0, N=3

| File | LLPO | File | LLPO |
|--------|-----------|---------|-----------|
| BEN_0 | -2.544323 | MWOR_0 | -2.402998 |
| BEN_1 | -2.64357 | MWOR_1 | -2.486666 |
| BEN_2 | -2.843443 | MWOR_2 | -2.504983 |
| BEN_3 | -2.608455 | MWOR_3 | -2.541051 |
| BEN_4 | -2.625266 | MWOR_4 | -2.4218 |
| BEN_5 | -2.619258 | MWOR_5 | -2.517544 |
| BEN_6 | -2.62047 | MWOR_6 | -2.382393 |
| BEN_7 | -2.84105 | MWOR_7 | -2.395489 |
| BEN_8 | -2.515048 | MWOR_8 | -2.49441 |
| BEN_9 | -2.669118 | MWOR_9 | -2.393952 |
| BEN_10 | -2.689387 | MWOR_10 | -2.380322 |
| BEN_11 | -2.526972 | MWOR_11 | -2.444773 |
| BEN_12 | -2.576147 | MWOR_12 | -2.421168 |
| BEN_13 | -2.478839 | MWOR_13 | -2.325241 |
| BEN_14 | -2.567223 | MWOR_14 | -2.527484 |
| BEN_15 | -2.690124 | MWOR_15 | -2.453113 |
| BEN_16 | -2.558649 | MWOR_16 | -2.353091 |
| BEN_17 | -2.451643 | MWOR_17 | -2.486506 |
| BEN_18 | -2.515152 | MWOR_18 | -2.45853 |
| BEN_19 | -2.560068 | MWOR_19 | -2.434684 |

Table D.3: LLPO scores - Worm-padding ratio: 4.0, N=3

| File | LLPO | File | LLPO |
|--------|-----------|---------|-----------|
| BEN_0 | -2.563521 | MWOR_0 | -2.478913 |
| BEN_1 | -2.652861 | MWOR_1 | -2.569835 |
| BEN_2 | -2.87828 | MWOR_2 | -2.502876 |
| BEN_3 | -2.606329 | MWOR_3 | -2.440894 |
| BEN_4 | -2.639205 | MWOR_4 | -2.326988 |
| BEN_5 | -2.633219 | MWOR_5 | -2.557039 |
| BEN_6 | -2.650461 | MWOR_6 | -2.465314 |
| BEN_7 | -2.878112 | MWOR_7 | -2.497504 |
| BEN_8 | -2.54517 | MWOR_8 | -2.391017 |
| BEN_9 | -2.665605 | MWOR_9 | -2.486907 |
| BEN_10 | -2.717854 | MWOR_10 | -2.448817 |
| BEN_11 | -2.543789 | MWOR_11 | -2.511273 |
| BEN_12 | -2.579349 | MWOR_12 | -2.522425 |
| BEN_13 | -2.477433 | MWOR_13 | -2.495827 |
| BEN_14 | -2.569425 | MWOR_14 | -2.392941 |
| BEN_15 | -2.714744 | MWOR_15 | -2.411323 |
| BEN_16 | -2.562329 | MWOR_16 | -2.718673 |
| BEN_17 | -2.455398 | MWOR_17 | -2.545033 |
| BEN_18 | -2.546387 | MWOR_18 | -2.552821 |
| BEN_19 | -2.581043 | MWOR_19 | -2.588134 |

APPENDIX E

Selected HMM Models

Table E.1: HMM matrices, N = 2 Worm-padding ratio: 2.0

| HMM Parameters | | |
|----------------------------|------------------------------|------------------------------|
| N = 2, M = 131, T = 790441 | | |
| π : | 0.0000000000 | 1.0000000000 |
| A : | 0.8874284727 0.0616794013 | 0.1125715273 0.9383205987 |
| B : | | |
| adc | 0.0000962463 | 0.0000060150 |
| add | 0.0223048733 | 0.0987331347 |
| addsd | 0.0001501143 | 0.0000000000 |
| addss | 0.0001358177 | 0.0000000000 |
| and | 0.0117147309 | 0.0357255629 |
| bsf | 0.0000500381 | 0.0000000000 |
| bsr | 0.0000030630 | 0.0000061549 |
| bswap | 0.0000000000 | 0.0000019583 |
| bt | 0.0001501143 | 0.0000000000 |
| call | 0.0497101214 | 0.0723558852 |
| cdqe | 0.0001440348 | 0.0065772642 |
| clc | 0.0000000000 | 0.0000058748 |
| cld | 0.0000000000 | 0.0000039166 |
| cmova | 0.0001165807 | 0.0000908293 |
| cmovae | 0.0002358939 | 0.0000000000 |
| cmovb | 0.0002823578 | 0.0000000000 |
| cmovbe | 0.0001608367 | 0.0000000000 |
| cmove | 0.0035955949 | 0.0000000000 |
| cmovg | 0.0001858558 | 0.0000000000 |
| cmovge | 0.0000929279 | 0.0000000000 |
| cmovl | 0.0000655234 | 0.0000013070 |
| cmovle | 0.0000857796 | 0.0000000000 |
| cmovne | 0.0018192423 | 0.0000000000 |
| cmovns | 0.0000718093 | 0.0000331119 |
| cmovs | 0.0001574846 | 0.0000018366 |
| cmp | 0.1287337339 | 0.0000000000 |
| cpuid | 0.0000986223 | 0.0000223376 |
| cvtssi2sd | 0.0002358939 | 0.0000000000 |
| cvtssi2ss | 0.0002501905 | 0.0000000000 |
| cvttsd2si | 0.0000142966 | 0.0000000000 |
| cvttss2si | 0.0000786313 | 0.0000000000 |
| Continued on Next Page... | | |

Table E.1 – Continued

| HMM Parameters | | |
|-----------------------|--------------|--------------|
| cwde | 0.0000000000 | 0.0000567900 |
| dec | 0.0000000000 | 0.0002898249 |
| div | 0.0003694867 | 0.0002401287 |
| divsd | 0.0000714830 | 0.0000000000 |
| divss | 0.0000107224 | 0.0000000000 |
| enter | 0.0000000000 | 0.0000391655 |
| fcmovnb | 0.0000000000 | 0.0000058748 |
| fild | 0.0000008404 | 0.0000112892 |
| fisttp | 0.0000084592 | 0.0000345307 |
| fld | 0.0000142966 | 0.0000000000 |
| fmul | 0.0000000000 | 0.0000176245 |
| fstp | 0.0000076758 | 0.0000075441 |
| fsub | 0.0000000000 | 0.0000019583 |
| fucomip | 0.0000071483 | 0.0000000000 |
| fxch | 0.0000071483 | 0.0000000000 |
| hlt | 0.0000000000 | 0.0000391655 |
| icebp | 0.0000000000 | 0.0000372072 |
| idiv | 0.0000000000 | 0.001351211 |
| imul | 0.0007768793 | 0.0012937144 |
| in | 0.0000144056 | 0.0000371475 |
| inc | 0.0001104452 | 0.000088311 |
| ja | 0.0083456402 | 0.0000000000 |
| jae | 0.0042246453 | 0.0000000000 |
| jb | 0.0049823651 | 0.0000000000 |
| jbe | 0.0064549149 | 0.0000000000 |
| je | 0.1199091576 | 0.0000000000 |
| jg | 0.0046928589 | 0.0000000000 |
| jge | 0.0009828912 | 0.0000000000 |
| jl | 0.0025805363 | 0.0000000000 |
| jle | 0.0076379585 | 0.0000000000 |
| jmp | 0.0383346104 | 0.0411913252 |
| jne | 0.0723836853 | 0.0000000000 |
| jnp | 0.0000107224 | 0.0000000000 |
| jns | 0.0011747288 | 0.0000025974 |
| jo | 0.0000030633 | 0.0000120296 |
| jp | 0.0000107224 | 0.0000000000 |
| js | 0.0035705758 | 0.0000000000 |
| ldmxcsr | 0.0000000000 | 0.0000019583 |
| lea | 0.0212980591 | 0.0262488989 |
| leave | 0.0000128848 | 0.0005765067 |
| lock | 0.0000000000 | 0.0000744145 |
| lod\$ | 0.0000000000 | 0.0000019583 |
| loop | 0.0000008308 | 0.0000073779 |
| loope | 0.0001644109 | 0.0000000000 |
| loopne | 0.0000026619 | 0.0000690395 |
| mov | 0.2512854820 | 0.4841948314 |
| movabs | 0.0009057861 | 0.0002184908 |
| movapd | 0.0000536122 | 0.0000000000 |
| movaps | 0.0000019070 | 0.0019023996 |

Continued on Next Page...

Table E.1 – Continued

| HMM Parameters | | |
|-----------------------|--------------|--------------|
| movs | 0.0000000000 | 0.0000469986 |
| movsd | 0.0007255524 | 0.0000000000 |
| movss | 0.0000929279 | 0.0000000000 |
| movsx | 0.0016784643 | 0.0004472465 |
| movsxd | 0.0014446895 | 0.0218715853 |
| movzx | 0.0252677456 | 0.0034297606 |
| mul | 0.0000422668 | 0.0000473400 |
| mulsd | 0.0000643347 | 0.0000000000 |
| mulss | 0.0001143728 | 0.0000000000 |
| neg | 0.0004151083 | 0.0003600451 |
| nop | 0.0265848542 | 0.0158442338 |
| not | 0.0005018279 | 0.0011761312 |
| or | 0.0046880928 | 0.0027716139 |
| out | 0.0000030457 | 0.0000218306 |
| pop | 0.0000000000 | 0.0222518925 |
| push | 0.0003771502 | 0.0203160941 |
| rep | 0.0003791506 | 0.0013158023 |
| repnz | 0.0000408011 | 0.0006473755 |
| repz | 0.0043506278 | 0.0000014721 |
| ret | 0.0007408776 | 0.0118332996 |
| retf | 0.0000000000 | 0.0000019583 |
| rex | 0.0000060341 | 0.0000064853 |
| rol | 0.0000000000 | 0.0004797777 |
| ror | 0.0000000000 | 0.0003485732 |
| sar | 0.0000172454 | 0.0019762433 |
| sbb | 0.0013464675 | 0.0000024991 |
| seta | 0.0008113320 | 0.0000000000 |
| setae | 0.0000178707 | 0.0000000000 |
| setb | 0.0007219783 | 0.0000000000 |
| setbe | 0.0000679088 | 0.0000000000 |
| sete | 0.0032238833 | 0.0000000000 |
| setg | 0.0001572626 | 0.0000000000 |
| setge | 0.0000571864 | 0.0000000000 |
| setl | 0.0000571864 | 0.0000000000 |
| setle | 0.0000428898 | 0.0000000000 |
| setne | 0.0030308792 | 0.0000000000 |
| sets | 0.0000071483 | 0.0000000000 |
| shl | 0.0000581400 | 0.0207474139 |
| shr | 0.0018454119 | 0.0026822080 |
| sldt | 0.0000035741 | 0.0000000000 |
| stmxcsr | 0.0000000000 | 0.0000019583 |
| stos | 0.0001143245 | 0.0000744409 |
| sub | 0.0106511885 | 0.0303884087 |
| subsd | 0.0000071483 | 0.0000000000 |
| subss | 0.0000393156 | 0.0000000000 |
| test | 0.1085183416 | 0.0000000000 |
| ucomisd | 0.0000428898 | 0.0000000000 |
| ucomiss | 0.0001965782 | 0.0000000000 |
| xchg | 0.0030175557 | 0.0010706439 |

Continued on Next Page...

Table E.1 – Continued

| HMM Parameters | | |
|-----------------------|--------------|--------------|
| xor | 0.0272213666 | 0.0694342484 |
| xorpd | 0.0000428898 | 0.0000000000 |

Table E.2: HMM matrices, N = 3 Worm-padding ratio: 2.0

| HMM Parameters | | | |
|----------------------------|--------------|--------------|--------------|
| N = 3, M = 131, T = 790441 | | | |
| π : | 0.0000000000 | 0.0000000000 | 1.0000000000 |
| A : | | | |
| | 0.8612819278 | 0.1372622966 | 0.0014557756 |
| | 0.0000012331 | 0.7801870820 | 0.2198116849 |
| | 0.5001390860 | 0.4998609140 | 0.0000000000 |
| B : | | | |
| adc | 0.0000828834 | 0.0000105444 | 0.0000000000 |
| add | 0.0234782893 | 0.0912150386 | 0.1570662990 |
| addsd | 0.0001345659 | 0.0000000000 | 0.0000000000 |
| addss | 0.0001217501 | 0.0000000000 | 0.0000000000 |
| and | 0.0085665320 | 0.0350832625 | 0.0589494082 |
| bsf | 0.0000000000 | 0.0000000000 | 0.0001617223 |
| bsr | 0.0000128158 | 0.0000000000 | 0.0000000000 |
| bswap | 0.0000000000 | 0.0000025526 | 0.0000000000 |
| bt | 0.0000580231 | 0.0000000000 | 0.0002759692 |
| call | 0.0104884193 | 0.0033310490 | 0.5345897198 |
| cdqe | 0.0001669943 | 0.0083739393 | 0.0007661987 |
| clc | 0.0000000000 | 0.0000076578 | 0.0000000000 |
| cld | 0.0000000000 | 0.0000051052 | 0.0000000000 |
| cmova | 0.0002531120 | 0.0000000000 | 0.0000000000 |
| cmovae | 0.0002070472 | 0.0000035163 | 0.0000000000 |
| cmovb | 0.0002531120 | 0.0000000000 | 0.0000000000 |
| cmovbe | 0.0000776469 | 0.0000530054 | 0.0000000000 |
| cmove | 0.0029079862 | 0.0002511113 | 0.0000000000 |
| cmovg | 0.0001323610 | 0.0000272827 | 0.0000000000 |
| cmovge | 0.0000833027 | 0.0000000000 | 0.0000000000 |
| cmovl | 0.0000532171 | 0.0000061011 | 0.0000000000 |
| cmovle | 0.0000707234 | 0.0000049168 | 0.0000000000 |
| cmovne | 0.0014605853 | 0.0001356193 | 0.0000000000 |
| cmovns | 0.0000701355 | 0.0000385690 | 0.0000000000 |
| cmovs | 0.0001431256 | 0.0000008383 | 0.0000000000 |
| cmp | 0.1070266756 | 0.0000000000 | 0.0301889020 |
| cpuid | 0.0000287684 | 0.0000000000 | 0.0003467898 |
| cvtssi2sd | 0.0002114607 | 0.0000000000 | 0.0000000000 |
| cvtssi2ss | 0.0002242765 | 0.0000000000 | 0.0000000000 |
| cvttsd2si | 0.0000128158 | 0.0000000000 | 0.0000000000 |
| cvttss2si | 0.0000704869 | 0.0000000000 | 0.0000000000 |
| cwde | 0.0000000000 | 0.0000740255 | 0.0000000000 |
| dec | 0.0000099010 | 0.0003105508 | 0.0002685659 |
| div | 0.0000336322 | 0.0000000000 | 0.0024894014 |
| divsd | 0.0000582197 | 0.0000046682 | 0.0000000000 |
| divss | 0.0000096118 | 0.0000000000 | 0.0000000000 |
| enter | 0.0000000000 | 0.0000510520 | 0.0000000000 |
| fcmovnb | 0.0000000000 | 0.0000076578 | 0.0000000000 |

Continued on Next Page...

Table E.2 – Continued

| HMM Parameters | | | |
|-----------------------|--------------|--------------|--------------|
| fild | 0.0000000000 | 0.0000153156 | 0.0000000000 |
| fisttp | 0.0000010288 | 0.0000152854 | 0.0001581495 |
| fld | 0.0000128158 | 0.0000000000 | 0.0000000000 |
| fmul | 0.0000000000 | 0.0000229734 | 0.0000000000 |
| fstp | 0.0000071958 | 0.0000095827 | 0.0000000000 |
| fsub | 0.0000032039 | 0.0000000000 | 0.0000000000 |
| fucomp | 0.0000064079 | 0.0000000000 | 0.0000000000 |
| fxch | 0.0000064079 | 0.0000000000 | 0.0000000000 |
| hlt | 0.0000640790 | 0.0000000000 | 0.0000000000 |
| icebp | 0.0000000000 | 0.0000484994 | 0.0000000000 |
| idiv | 0.0000000000 | 0.0000000000 | 0.0007970598 |
| imul | 0.0006132673 | 0.0015983244 | 0.0006981240 |
| in | 0.0000167522 | 0.0000453633 | 0.0000000000 |
| inc | 0.0000835692 | 0.0000559938 | 0.0003232233 |
| ja | 0.0074812232 | 0.0000000000 | 0.0000000000 |
| jae | 0.0037870689 | 0.0000000000 | 0.0000000000 |
| jb | 0.0044663063 | 0.0000000000 | 0.0000000000 |
| jbe | 0.0057863337 | 0.0000000000 | 0.0000000000 |
| je | 0.1074893184 | 0.0000000000 | 0.0000000000 |
| jg | 0.0042067863 | 0.0000000000 | 0.0000000000 |
| jge | 0.0008466299 | 0.0000274515 | 0.0000000000 |
| jl | 0.0023132519 | 0.0000000000 | 0.0000000000 |
| jle | 0.0068468411 | 0.0000000000 | 0.0000000000 |
| jmp | 0.0656506094 | 0.0116690931 | 0.0773728756 |
| jne | 0.0648863953 | 0.0000000000 | 0.0000000000 |
| jnp | 0.0000096118 | 0.0000000000 | 0.0000000000 |
| jns | 0.0007665269 | 0.0002316631 | 0.0000000000 |
| jo | 0.0000001864 | 0.0000177197 | 0.0000000000 |
| jp | 0.0000096118 | 0.0000000000 | 0.0000000000 |
| js | 0.0032007460 | 0.0000000000 | 0.0000000000 |
| ldmxcsr | 0.0000032039 | 0.0000000000 | 0.0000000000 |
| lea | 0.0159713702 | 0.0362829569 | 0.0018943892 |
| leave | 0.0005994922 | 0.0000000000 | 0.0012809520 |
| lock | 0.0000051874 | 0.0000397825 | 0.0002402252 |
| lod\$ | 0.0000000000 | 0.0000025526 | 0.0000000000 |
| loop | 0.0000000000 | 0.0000102104 | 0.0000000000 |
| loope | 0.0000000000 | 0.0000000000 | 0.0005313732 |
| loopne | 0.0000042639 | 0.0000884966 | 0.0000000000 |
| mov | 0.2228118157 | 0.6235781612 | 0.0430640170 |
| movabs | 0.0007338803 | 0.0002167839 | 0.0005893452 |
| movapd | 0.0000480592 | 0.0000000000 | 0.0000000000 |
| movaps | 0.0031142394 | 0.0000000000 | 0.0000000000 |
| movs | 0.0000000000 | 0.0000002543 | 0.0002760874 |
| movsd | 0.0002950718 | 0.0002830931 | 0.0000000000 |
| movss | 0.0000833027 | 0.0000000000 | 0.0000000000 |
| movsx | 0.0013002940 | 0.0007457659 | 0.0000000000 |
| movsxd | 0.0012559968 | 0.0284969571 | 0.0001975253 |
| movzx | 0.0224119768 | 0.0019835049 | 0.0121157674 |
| mul | 0.0000000000 | 0.0000918937 | 0.0000000000 |

Continued on Next Page...

Table E.2 – Continued

| HMM Parameters | | | |
|-----------------------|---------------|--------------|--------------|
| mulsd | 0.0000576711 | 0.0000000000 | 0.0000000000 |
| mulss | 0.0001025264 | 0.0000000000 | 0.0000000000 |
| neg | 0.0004132444 | 0.0003309115 | 0.0004780444 |
| nop | 0.0487322115 | 0.0008141748 | 0.0000000000 |
| not | 0.0001655860 | 0.0010675424 | 0.0031316466 |
| or | 0.0051077514 | 0.0014539539 | 0.0065058417 |
| out | 0.0000000000 | 0.0000306312 | 0.0000000000 |
| pop | 0.0364064838 | 0.0000000000 | 0.0000000000 |
| push | 0.0335773960 | 0.0000000000 | 0.0000000000 |
| rep | 0.0002909919 | 0.0012972864 | 0.0020672262 |
| repnz | 0.0000000000 | 0.0008088005 | 0.0002904841 |
| repz | 0.0017800704 | 0.0000000000 | 0.0076519334 |
| ret | 0.0200243835 | 0.0000002422 | 0.0000000000 |
| retf | 0.0000000000 | 0.0000025526 | 0.0000000000 |
| rex | 0.00000030712 | 0.0000000000 | 0.0000466851 |
| rol | 0.0000042868 | 0.0005870880 | 0.0001578656 |
| ror | 0.0000031970 | 0.0003717528 | 0.0003623200 |
| sar | 0.0000170744 | 0.0023766679 | 0.0008963376 |
| sbb | 0.0007386885 | 0.0003763670 | 0.0000000000 |
| seta | 0.0007272966 | 0.0000000000 | 0.0000000000 |
| setae | 0.0000160197 | 0.0000000000 | 0.0000000000 |
| setb | 0.0006471979 | 0.0000000000 | 0.0000000000 |
| setbe | 0.00000608750 | 0.0000000000 | 0.0000000000 |
| sete | 0.0028381179 | 0.0000413051 | 0.0000000000 |
| setg | 0.0001409738 | 0.0000000000 | 0.0000000000 |
| setge | 0.0000512632 | 0.0000000000 | 0.0000000000 |
| setl | 0.0000512632 | 0.0000000000 | 0.0000000000 |
| setle | 0.00000384474 | 0.0000000000 | 0.0000000000 |
| setne | 0.0027169496 | 0.0000000000 | 0.0000000000 |
| sets | 0.0000064079 | 0.0000000000 | 0.0000000000 |
| shl | 0.0002439713 | 0.0264287036 | 0.0020933850 |
| shr | 0.0004962522 | 0.0025269726 | 0.0085614955 |
| sldt | 0.0000032039 | 0.0000000000 | 0.0000000000 |
| stmxcsr | 0.0000032039 | 0.0000000000 | 0.0000000000 |
| stos | 0.0001597281 | 0.0000000000 | 0.0002327241 |
| sub | 0.0128469226 | 0.0288366179 | 0.0368650112 |
| subsd | 0.0000064079 | 0.0000000000 | 0.0000000000 |
| subss | 0.0000352434 | 0.0000000000 | 0.0000000000 |
| test | 0.0972783254 | 0.0000000000 | 0.0000000158 |
| ucomisd | 0.0000384474 | 0.0000000000 | 0.0000000000 |
| ucomiss | 0.0001762172 | 0.0000000000 | 0.0000000000 |
| xchg | 0.0043416162 | 0.0000916833 | 0.0000000000 |
| xor | 0.0259037597 | 0.0879810038 | 0.0060168932 |
| xorpd | 0.0000384474 | 0.0000000000 | 0.0000000000 |

Table E.3: HMM matrices, N = 2 Worm-padding ratio: 3.0

| HMM Parameters | | |
|-----------------------------|--------------|--------------|
| N = 2, M = 129, T = 1054041 | | |
| π : | 1.0000000000 | 0.0000000000 |
| A : | | |
| | 0.8798421953 | 0.1201578047 |
| | 0.0679607327 | 0.9320392673 |
| B : | | |
| adc | 0.0000623653 | 0.0000048299 |
| add | 0.0227135425 | 0.0838085640 |
| addsd | 0.0001785745 | 0.0000000000 |
| addss | 0.0001024178 | 0.0000000000 |
| and | 0.0101517075 | 0.0283808283 |
| bsf | 0.0000105044 | 0.0000000000 |
| bsr | 0.0000000000 | 0.0000118827 |
| bswap | 0.0000000000 | 0.0000089120 |
| bt | 0.0002074616 | 0.0000000000 |
| call | 0.0507969274 | 0.0820009550 |
| cdqe | 0.0002427649 | 0.0051029690 |
| clc | 0.0000000000 | 0.0000044560 |
| cld | 0.0000000000 | 0.0000029707 |
| cmova | 0.0001001587 | 0.0001899159 |
| cmovae | 0.0002337226 | 0.0000000000 |
| cmovb | 0.0002704879 | 0.0000000000 |
| cmovbe | 0.0003256359 | 0.0000000000 |
| cmove | 0.0036213866 | 0.0000000000 |
| cmovg | 0.0001654441 | 0.0000000000 |
| cmovge | 0.0001129221 | 0.0000000000 |
| cmovl | 0.0000459651 | 0.0000022233 |
| cmovle | 0.0001127475 | 0.0000015841 |
| cmovne | 0.0019932070 | 0.0000000000 |
| cmovns | 0.0001055527 | 0.0000115949 |
| cmovs | 0.0001024178 | 0.0000000000 |
| cmp | 0.1283557032 | 0.0000000000 |
| cpuid | 0.0000394959 | 0.0000103383 |
| cvttsi2sd | 0.0002888706 | 0.0000000000 |
| cvttsi2ss | 0.0001864528 | 0.0000000000 |
| cvttsd2si | 0.0000105044 | 0.0000000000 |
| cvttss2si | 0.0000604002 | 0.0000000000 |
| cwde | 0.0000000000 | 0.0000430749 |
| dec | 0.0000000000 | 0.0002257716 |
| div | 0.0003908249 | 0.0003998185 |
| divsd | 0.0000919134 | 0.0000000000 |
| divss | 0.0000078783 | 0.0000000000 |
| enter | 0.0000000000 | 0.0000297068 |
| fcmovnb | 0.0000000000 | 0.0000044560 |
| fld | 0.0000000000 | 0.0000089120 |
| Continued on Next Page... | | |

Table E.3 – Continued

| HMM Parameters | | |
|----------------|--------------|--------------|
| fisttp | 0.0000056207 | 0.0000265277 |
| fld | 0.0000000000 | 0.0000059414 |
| fmul | 0.0000000000 | 0.0000133681 |
| fstp | 0.0000000000 | 0.0000089120 |
| fsub | 0.0000000000 | 0.0000014853 |
| fucomip | 0.0000000000 | 0.0000029707 |
| fxch | 0.0000000000 | 0.0000029707 |
| hlt | 0.0000000000 | 0.0000519869 |
| icebp | 0.0000000000 | 0.0000282215 |
| idiv | 0.0000000000 | 0.0000891204 |
| imul | 0.0005759725 | 0.0010778717 |
| in | 0.0000104706 | 0.0000282406 |
| inc | 0.0001209957 | 0.0000622738 |
| ja | 0.0092202237 | 0.0000000000 |
| jae | 0.0052837055 | 0.0000000000 |
| jb | 0.0059297252 | 0.0000000000 |
| jbe | 0.0069827898 | 0.0000000000 |
| je | 0.1258372769 | 0.0000000000 |
| jg | 0.0040993361 | 0.0000000000 |
| jge | 0.0011607345 | 0.0000000000 |
| jl | 0.0021849120 | 0.0000000000 |
| jle | 0.0070221812 | 0.0000000000 |
| jmp | 0.0264328267 | 0.0563145109 |
| jne | 0.0731735441 | 0.0000000000 |
| jnp | 0.0000052522 | 0.0000000000 |
| jns | 0.0011003343 | 0.0000000000 |
| jo | 0.0000022305 | 0.0000091358 |
| jp | 0.0000131305 | 0.0000000000 |
| js | 0.0039522748 | 0.0000000000 |
| lea | 0.0261441439 | 0.0277409236 |
| leave | 0.0000073980 | 0.0004429029 |
| lock | 0.0000000000 | 0.0000564429 |
| lod\$ | 0.0000000000 | 0.0000014853 |
| loop | 0.0000002381 | 0.0000058067 |
| loope | 0.0001208004 | 0.0000000000 |
| loopne | 0.0000016139 | 0.0000525594 |
| mov | 0.2556700975 | 0.4798947462 |
| movabs | 0.0008012547 | 0.0003503732 |
| movapd | 0.0000656524 | 0.0000000000 |
| movaps | 0.0000000000 | 0.0013724539 |
| movs | 0.0000000000 | 0.0000415895 |
| movsd | 0.0001582972 | 0.0003471558 |
| movss | 0.0000682785 | 0.0000000000 |
| movsx | 0.0019355024 | 0.0004529893 |
| movsxd | 0.0015610365 | 0.0177372853 |
| movzx | 0.0241815988 | 0.0039893369 |
| mul | 0.0000261068 | 0.0001545625 |
| mulsd | 0.0000814090 | 0.0000000000 |
| mulss | 0.0000840351 | 0.0000000000 |

Continued on Next Page...

Table E.3 – Continued

| HMM Parameters | | |
|----------------|--------------|--------------|
| neg | 0.0002820293 | 0.0005088850 |
| nop | 0.0204647588 | 0.0207444864 |
| not | 0.0003899404 | 0.0011400180 |
| or | 0.0034646895 | 0.0030073217 |
| out | 0.0000024414 | 0.0000164432 |
| pop | 0.0000000000 | 0.0241991554 |
| push | 0.0002968426 | 0.0227583229 |
| rep | 0.0005232092 | 0.0010483014 |
| repnz | 0.0000000000 | 0.0005867092 |
| repz | 0.0054341312 | 0.0000144358 |
| ret | 0.0001471499 | 0.0123535208 |
| retf | 0.0000000000 | 0.0000014853 |
| rex | 0.0000000050 | 0.0000074239 |
| rol | 0.0000000000 | 0.0004010417 |
| ror | 0.0000000000 | 0.0002643905 |
| sar | 0.0000069096 | 0.0016210536 |
| sbb | 0.0018810120 | 0.0000129568 |
| seta | 0.0010425602 | 0.0000000000 |
| setae | 0.0000262610 | 0.0000000000 |
| setb | 0.0009322641 | 0.0000000000 |
| setbe | 0.0000446436 | 0.0000000000 |
| sete | 0.0033640292 | 0.0000000000 |
| setg | 0.0001549397 | 0.0000000000 |
| setge | 0.0000315132 | 0.0000000000 |
| setl | 0.0000367653 | 0.0000000000 |
| setle | 0.0000236349 | 0.0000000000 |
| setne | 0.0024370173 | 0.0000000000 |
| sets | 0.0000078783 | 0.0000000000 |
| shl | 0.0000661565 | 0.0172875844 |
| shr | 0.0019120854 | 0.0025902700 |
| sldt | 0.0000026261 | 0.0000000000 |
| stos | 0.0000490186 | 0.0000287176 |
| sub | 0.0099482600 | 0.0266941826 |
| subsd | 0.0000052522 | 0.0000000000 |
| subss | 0.0000288871 | 0.0000000000 |
| test | 0.1157478154 | 0.0000000000 |
| ucomisd | 0.0000315132 | 0.0000000000 |
| ucomiss | 0.0001444353 | 0.0000000000 |
| xchg | 0.0025051041 | 0.0014601974 |
| xor | 0.0234487579 | 0.0726254926 |
| xorpd | 0.0000065047 | 0.0000096890 |

Table E.4: HMM matrices, N = 3 Worm-padding ratio: 3.0

| HMM Parameters | | | |
|-----------------------------|--------------|--------------|--------------|
| N = 3, M = 129, T = 1054041 | | | |
| π : | 1.0000000000 | 0.0000000000 | 0.0000000000 |
| A : | | | |
| | 0.8401558381 | 0.1184121543 | 0.0414320076 |
| | 0.0871060187 | 0.8805817832 | 0.0323121981 |
| | 0.0544288643 | 0.0613836061 | 0.8841875296 |
| B : | | | |
| adc | 0.0000686927 | 0.0000000000 | 0.0000149139 |
| add | 0.0280699091 | 0.0174225388 | 0.1893056150 |
| addsd | 0.0002008214 | 0.0000000000 | 0.0000000000 |
| addss | 0.0001151770 | 0.0000000000 | 0.0000000000 |
| and | 0.0112359283 | 0.0138288670 | 0.0508137537 |
| bsf | 0.0000118130 | 0.0000000000 | 0.0000000000 |
| bsr | 0.0000000000 | 0.0000000000 | 0.0000319014 |
| bswap | 0.0000000000 | 0.0000129127 | 0.0000000000 |
| bt | 0.0002333073 | 0.0000000000 | 0.0000000000 |
| call | 0.0325833308 | 0.1354266373 | 0.0023525599 |
| cdqe | 0.0002378837 | 0.0047539025 | 0.0049387804 |
| clc | 0.0000000000 | 0.0000000000 | 0.0000119630 |
| cld | 0.0000000000 | 0.0000000000 | 0.0000079753 |
| cmova | 0.0001009336 | 0.0000000000 | 0.0005256663 |
| cmovae | 0.0002628398 | 0.0000000000 | 0.0000000000 |
| cmovb | 0.0003041854 | 0.0000000000 | 0.0000000000 |
| cmovbe | 0.0003276320 | 0.0000281084 | 0.0000000000 |
| cmove | 0.0040670800 | 0.0000000010 | 0.0000073716 |
| cmovg | 0.0001792889 | 0.0000049308 | 0.0000000000 |
| cmovge | 0.0001269900 | 0.0000000000 | 0.0000000000 |
| cmovl | 0.0000497627 | 0.0000046268 | 0.0000000000 |
| cmovle | 0.0001186605 | 0.0000000000 | 0.0000152347 |
| cmovne | 0.0021607049 | 0.0000588935 | 0.0000000000 |
| cmovns | 0.0001138984 | 0.0000012441 | 0.0000353103 |
| cmovs | 0.0001151770 | 0.0000000000 | 0.0000000000 |
| cmp | 0.1443463177 | 0.0000000000 | 0.0000000000 |
| cpuid | 0.0000336036 | 0.0000163412 | 0.0000120764 |
| cvtssi2sd | 0.0003248582 | 0.0000000000 | 0.0000000000 |
| cvtssi2ss | 0.0002096812 | 0.0000000000 | 0.0000000000 |
| cvttsd2si | 0.0000118130 | 0.0000000000 | 0.0000000000 |
| cvttss2si | 0.0000679249 | 0.0000000000 | 0.0000000000 |
| cwde | 0.0000000000 | 0.0000025685 | 0.0001108831 |
| dec | 0.0000485819 | 0.0000246204 | 0.0004949083 |
| div | 0.0003450119 | 0.0003707240 | 0.0005140745 |
| divsd | 0.0001033640 | 0.0000000000 | 0.0000000000 |
| divss | 0.0000088598 | 0.0000000000 | 0.0000000000 |
| enter | 0.0000000000 | 0.0000000000 | 0.0000797534 |
| fcmovnb | 0.0000000000 | 0.0000023113 | 0.0000076803 |

Continued on Next Page...

Table E.4 – Continued

| HMM Parameters | | | |
|-----------------------|--------------|--------------|--------------|
| fild | 0.0000000000 | 0.0000000000 | 0.0000239260 |
| fisttp | 0.0000088875 | 0.0000000000 | 0.0000677530 |
| fld | 0.0000118130 | 0.0000000000 | 0.0000000000 |
| fmul | 0.0000000000 | 0.0000017796 | 0.0000325916 |
| fstp | 0.0000065920 | 0.0000000000 | 0.0000150251 |
| fsub | 0.0000000000 | 0.0000000000 | 0.0000039877 |
| fucomp | 0.0000059065 | 0.0000000000 | 0.0000000000 |
| fxch | 0.0000059065 | 0.0000000000 | 0.0000000000 |
| hlt | 0.0000000000 | 0.0000730641 | 0.0000041878 |
| icebp | 0.0000000000 | 0.0000000000 | 0.0000757657 |
| idiv | 0.0000000000 | 0.0000000000 | 0.0002392601 |
| imul | 0.0006387832 | 0.0005153713 | 0.0019508906 |
| in | 0.0000123661 | 0.0000000000 | 0.0000750190 |
| inc | 0.0001379581 | 0.0000300376 | 0.0001089787 |
| ja | 0.0103688836 | 0.0000000000 | 0.0000000000 |
| jae | 0.0059419521 | 0.0000000000 | 0.0000000000 |
| jb | 0.0066684532 | 0.0000000000 | 0.0000000000 |
| jbe | 0.0078527090 | 0.0000000000 | 0.0000000000 |
| je | 0.1415141447 | 0.0000000000 | 0.0000000000 |
| jg | 0.0046100334 | 0.0000000000 | 0.0000000000 |
| jge | 0.0013053394 | 0.0000000000 | 0.0000000000 |
| jl | 0.0024571094 | 0.0000000000 | 0.0000000000 |
| jle | 0.0078970079 | 0.0000000000 | 0.0000000000 |
| jmp | 0.0221411910 | 0.0608761139 | 0.0486305594 |
| jne | 0.0822895390 | 0.0000000000 | 0.0000000000 |
| jnp | 0.0000059065 | 0.0000000000 | 0.0000000000 |
| jns | 0.0011172046 | 0.0000824689 | 0.0000095080 |
| jo | 0.0000025507 | 0.0000000000 | 0.0000244696 |
| jp | 0.0000147663 | 0.0000000000 | 0.0000000000 |
| js | 0.0044416529 | 0.0000000000 | 0.0000040482 |
| lea | 0.0207468819 | 0.0374799817 | 0.0167145260 |
| leave | 0.0000048021 | 0.0000000000 | 0.0011938042 |
| lock | 0.0000000000 | 0.0000041588 | 0.0001438256 |
| lod | 0.0000000000 | 0.0000000000 | 0.0000039877 |
| loop | 0.0000000000 | 0.0000000000 | 0.0000159507 |
| loope | 0.0001358498 | 0.0000000000 | 0.0000000000 |
| loopne | 0.0000020400 | 0.0000000000 | 0.0001408015 |
| mov | 0.2143872020 | 0.5913503857 | 0.2914029817 |
| movabs | 0.0008978493 | 0.0001832596 | 0.0006054355 |
| movapd | 0.0000738314 | 0.0000000000 | 0.0000000000 |
| movaps | 0.0027288090 | 0.0000000000 | 0.0000000000 |
| movs | 0.0000000000 | 0.0000602594 | 0.0000000000 |
| movsd | 0.0001029955 | 0.0005576681 | 0.0000000000 |
| movss | 0.0000767847 | 0.0000000000 | 0.0000000000 |
| movsx | 0.0019227582 | 0.0004187492 | 0.0007830236 |
| movsxd | 0.0019069202 | 0.0036603345 | 0.0406323382 |
| movzx | 0.0262046980 | 0.0025548983 | 0.0073121624 |
| mul | 0.0000280977 | 0.0000086801 | 0.0004005715 |
| mulsd | 0.0000915510 | 0.0000000000 | 0.0000000000 |

Continued on Next Page...

Table E.4 – Continued

| HMM Parameters | | | |
|-----------------------|---------------|--------------|--------------|
| mulss | 0.0000945042 | 0.0000000000 | 0.0000000000 |
| neg | 0.0002366660 | 0.0005907692 | 0.0003802532 |
| nop | 0.0195140607 | 0.0202251175 | 0.0229434617 |
| not | 0.0004292780 | 0.0000000007 | 0.0030730658 |
| or | 0.0036517954 | 0.0013136726 | 0.0059697802 |
| out | 0.0000054794 | 0.0000000000 | 0.0000404534 |
| pop | 0.0000000000 | 0.0000000000 | 0.0649671000 |
| push | 0.0006618863 | 0.0000000000 | 0.0606559482 |
| rep | 0.0005787808 | 0.0014835884 | 0.0000783925 |
| repnz | 0.0000000000 | 0.0000000000 | 0.0015751292 |
| repz | 0.0059393660 | 0.0000000000 | 0.0002706657 |
| ret | 0.0002012314 | 0.0000000000 | 0.0331170357 |
| retf | 0.0000000000 | 0.0000000000 | 0.0000039877 |
| rex | 0.0000000000 | 0.0000000000 | 0.0000199383 |
| rol | 0.0000000000 | 0.0000000000 | 0.0010766706 |
| ror | 0.0000000000 | 0.0000000000 | 0.0007098050 |
| sar | 0.0000230304 | 0.0000793049 | 0.0041844685 |
| sbb | 0.0020508079 | 0.0000000000 | 0.0001219327 |
| seta | 0.0011724428 | 0.0000000000 | 0.0000000000 |
| setae | 0.0000295326 | 0.0000000000 | 0.0000000000 |
| setb | 0.0010484061 | 0.0000000000 | 0.0000000000 |
| setbe | 0.0000502054 | 0.0000000000 | 0.0000000000 |
| sete | 0.0037831216 | 0.0000000000 | 0.0000000000 |
| setg | 0.0001742421 | 0.0000000000 | 0.0000000000 |
| setge | 0.0000354391 | 0.0000000000 | 0.0000000000 |
| setl | 0.0000413456 | 0.0000000000 | 0.0000000000 |
| setle | 0.0000265793 | 0.0000000000 | 0.0000000000 |
| setne | 0.0027312174 | 0.0000000000 | 0.0000126987 |
| sets | 0.0000088598 | 0.0000000000 | 0.0000000000 |
| shl | 0.0004156036 | 0.0006030007 | 0.0448336949 |
| shr | 0.0022834459 | 0.0001579169 | 0.0064816637 |
| sldt | 0.00000029533 | 0.0000000000 | 0.0000000000 |
| stos | 0.0000513155 | 0.0000217031 | 0.0000420285 |
| sub | 0.0106269804 | 0.0145519773 | 0.0454590987 |
| subsd | 0.0000059065 | 0.0000000000 | 0.0000000000 |
| subss | 0.0000324858 | 0.0000000000 | 0.0000000000 |
| test | 0.1301007285 | 0.0000000000 | 0.0000904740 |
| ucomisd | 0.0000354391 | 0.0000000000 | 0.0000000000 |
| ucomiss | 0.0001624291 | 0.0000000000 | 0.0000000000 |
| xchg | 0.0026466208 | 0.0013329123 | 0.0016807297 |
| xor | 0.0161896499 | 0.0898088944 | 0.0423157229 |
| xorpd | 0.0000064034 | 0.0000147027 | 0.0000000000 |

Table E.5: HMM matrices, N = 2 Worm-padding ratio: 4.0

| HMM Parameters | | |
|-----------------------------|--------------|--------------|
| N = 2, M = 131, T = 1317049 | | |
| π : | 0.9985471245 | 0.0014528755 |
| A : | 0.4967575341 | 0.5032424659 |
| | 0.4597537055 | 0.5402462945 |
| B : | | |
| adc | 0.0000367951 | 0.0000375784 |
| add | 0.0547993781 | 0.0579618186 |
| addsd | 0.0000661023 | 0.0000572977 |
| addss | 0.0000206925 | 0.0000275895 |
| and | 0.0190965142 | 0.0186388023 |
| bsf | 0.0000024473 | 0.0000021230 |
| bsr | 0.0000055805 | 0.0000065252 |
| bswap | 0.0000111953 | 0.0000101133 |
| bt | 0.0000948431 | 0.0000949696 |
| call | 0.0731853855 | 0.0677838613 |
| cdqe | 0.0028501174 | 0.0030568097 |
| clc | 0.0000023837 | 0.0000021811 |
| cld | 0.0000014840 | 0.0000015501 |
| cmova | 0.0000823310 | 0.0001064005 |
| cmovae | 0.0000736147 | 0.0000736814 |
| cmovb | 0.0001471997 | 0.0001459370 |
| cmovbe | 0.0000909783 | 0.0000868770 |
| cmove | 0.0014361536 | 0.0014165634 |
| cmovg | 0.0000714001 | 0.0000757046 |
| cmovge | 0.0000405580 | 0.0000414053 |
| cmovl | 0.0000240547 | 0.0000230649 |
| cmovle | 0.0000500548 | 0.0000574291 |
| cmovne | 0.0008673460 | 0.0008029283 |
| cmovns | 0.0000718731 | 0.0000810842 |
| cmovs | 0.0000347324 | 0.0000321982 |
| cmp | 0.0515371734 | 0.0485093581 |
| cpuid | 0.0000189153 | 0.0000190427 |
| cvtssi2sd | 0.0001117871 | 0.0000867545 |
| cvtssi2ss | 0.0000409571 | 0.0000439466 |
| cvttsd2si | 0.0000034505 | 0.0000026595 |
| cvttss2si | 0.0000153175 | 0.0000150649 |
| cwde | 0.0000227074 | 0.0000213900 |
| dec | 0.0001377207 | 0.0001269911 |
| div | 0.0003169465 | 0.0003540926 |
| divsd | 0.0000369084 | 0.0000273043 |
| divss | 0.0000031685 | 0.0000029171 |
| enter | 0.0000144419 | 0.0000158648 |
| fcmovnb | 0.0000021302 | 0.0000024126 |
| fild | 0.0000041303 | 0.0000049443 |
| Continued on Next Page... | | |

Table E.5 – Continued

| HMM Parameters | | |
|-----------------------|--------------|---------------|
| fisttp | 0.0000141685 | 0.0000161146 |
| fld | 0.0000035138 | 0.0000026015 |
| fmul | 0.0000069576 | 0.0000067201 |
| fstp | 0.0000040950 | 0.0000049765 |
| fsub | 0.0000007945 | 0.0000007271 |
| fucomip | 0.0000013759 | 0.0000016489 |
| fxch | 0.0000015861 | 0.0000014568 |
| hlt | 0.0000444187 | 0.0000335194 |
| icebp | 0.0000148737 | 0.0000140174 |
| idiv | 0.0000676179 | 0.0000718953 |
| imul | 0.0011402858 | 0.0010969722 |
| in | 0.0000174705 | 0.0000174567 |
| inc | 0.0001124096 | 0.0001079798 |
| ja | 0.0030456559 | 0.0028665454 |
| jae | 0.0018727266 | 0.0018124722 |
| jb | 0.0019311099 | 0.0017097344 |
| jbe | 0.0025497522 | 0.0024056995 |
| je | 0.0523560313 | 0.0460758585 |
| jg | 0.0017213198 | 0.0014582503 |
| jge | 0.0005566059 | 0.0005100005 |
| jl | 0.0007592538 | 0.0007927095 |
| jle | 0.0027505774 | 0.0024459807 |
| jmp | 0.0414677057 | 0.0538642017 |
| jne | 0.0288874261 | 0.0282174391 |
| jnp | 0.0000016647 | 0.0000013851 |
| jns | 0.0004435686 | 0.0004272941 |
| jo | 0.0000053730 | 0.0000052619 |
| jp | 0.0000050735 | 0.0000040826 |
| js | 0.0014141650 | 0.0012070882 |
| ldmxcsr | 0.0000035979 | 0.0000039777 |
| lea | 0.0279573494 | 0.0268732118 |
| leave | 0.0002199441 | 0.0002465663 |
| lock | 0.0000309610 | 0.0000269260 |
| lod\$ | 0.0000005859 | 0.00000009177 |
| loop | 0.0000026285 | 0.0000034104 |
| loope | 0.0000345714 | 0.0000352511 |
| loopne | 0.0000245244 | 0.0000299006 |
| mov | 0.3930410177 | 0.3871306459 |
| movabs | 0.0004675989 | 0.0004867047 |
| movapd | 0.0000221904 | 0.0000233152 |
| movaps | 0.0010165383 | 0.0012797668 |
| movs | 0.0000502519 | 0.0000427197 |
| movsd | 0.0003220612 | 0.0002607909 |
| movss | 0.0000226994 | 0.0000228502 |
| movsx | 0.0012568459 | 0.0011110782 |
| movsxd | 0.0111392407 | 0.0106787844 |
| movzx | 0.0133626910 | 0.0112336983 |
| mul | 0.0000375296 | 0.0000427190 |
| mulsd | 0.0000254538 | 0.0000232397 |

Continued on Next Page...

Table E.5 – Continued

| HMM Parameters | | |
|-----------------------|--------------|--------------|
| mulss | 0.0000172847 | 0.0000190794 |
| neg | 0.0003653912 | 0.0003723104 |
| nop | 0.0196748718 | 0.0254666308 |
| not | 0.0011966786 | 0.0010381879 |
| or | 0.0038876450 | 0.0037187921 |
| out | 0.0000088417 | 0.0000093576 |
| pop | 0.0122520965 | 0.0199183607 |
| push | 0.0142035825 | 0.0186425878 |
| rep | 0.0008245629 | 0.0008115026 |
| repnz | 0.0005120233 | 0.0004257781 |
| repz | 0.0023332268 | 0.0019337110 |
| ret | 0.0071281524 | 0.0098289848 |
| retf | 0.0000008168 | 0.0000007067 |
| rex | 0.0000042149 | 0.0000034140 |
| rol | 0.0005261586 | 0.0004695289 |
| ror | 0.0001090077 | 0.0001604875 |
| sar | 0.0010894266 | 0.0012872768 |
| sbb | 0.0007413612 | 0.0006841036 |
| seta | 0.0004151954 | 0.0004009098 |
| setae | 0.0000139731 | 0.0000133872 |
| setb | 0.0003812304 | 0.0003825399 |
| setbe | 0.0000194379 | 0.0000214711 |
| sete | 0.0015104261 | 0.0013356327 |
| setg | 0.0000983457 | 0.0000917697 |
| setge | 0.0000185478 | 0.0000179254 |
| setl | 0.0000474728 | 0.0000467115 |
| setle | 0.0000150363 | 0.0000153217 |
| setne | 0.0011659902 | 0.0011330593 |
| sets | 0.0000036357 | 0.0000024902 |
| shl | 0.0089551704 | 0.0096462016 |
| shr | 0.0020773486 | 0.0024057586 |
| sldt | 0.0000007113 | 0.0000008031 |
| stmxcsr | 0.0000032987 | 0.0000042510 |
| stos | 0.0000627205 | 0.0000560284 |
| sub | 0.0212834226 | 0.0197007569 |
| subsd | 0.0000014974 | 0.0000015378 |
| subss | 0.0000070480 | 0.0000080904 |
| test | 0.0465648092 | 0.0429759322 |
| ucomisd | 0.0000119182 | 0.0000094528 |
| ucomiss | 0.0000456744 | 0.0000410899 |
| xchg | 0.0020071457 | 0.0019729912 |
| xor | 0.0547352782 | 0.0503183741 |
| xorpd | 0.0000144939 | 0.0000129114 |

Table E.6: HMM matrices, N = 3 Worm-padding ratio: 4.0

| HMM Parameters | | | |
|-----------------------------|---------------|--------------|--------------|
| N = 3, M = 131, T = 1317049 | | | |
| π : | 0.0000000000 | 0.0000000000 | 1.0000000000 |
| A : | | | |
| | 0.8440445378 | 0.1369401603 | 0.0190153020 |
| | 0.0020971899 | 0.5243338837 | 0.4735689264 |
| | 0.2700737983 | 0.4832011537 | 0.2467250480 |
| B : | | | |
| adc | 0.0000768630 | 0.0000154039 | 0.0000008589 |
| add | 0.0219442537 | 0.0418087140 | 0.1391768850 |
| addsd | 0.0001499633 | 0.0000000000 | 0.0000000000 |
| addss | 0.0000592448 | 0.0000000000 | 0.0000000000 |
| and | 0.0056939193 | 0.0163670891 | 0.0457075428 |
| bsf | 0.0000000000 | 0.0000000080 | 0.0000097197 |
| bsr | 0.0000148112 | 0.0000000000 | 0.0000000000 |
| bswap | 0.0000000000 | 0.0000229204 | 0.0000105699 |
| bt | 0.0002314242 | 0.0000000000 | 0.0000000012 |
| call | 0.0080288331 | 0.0040484733 | 0.2803971111 |
| cdqe | 0.0002383820 | 0.0065649974 | 0.0022401434 |
| clc | 0.0000000000 | 0.0000062093 | 0.0000002920 |
| cld | 0.0000000000 | 0.0000041118 | 0.0000002368 |
| cmova | 0.0002314248 | 0.0000000000 | 0.0000000000 |
| cmovae | 0.0001795857 | 0.0000000000 | 0.0000000000 |
| cmovb | 0.0003573199 | 0.0000000000 | 0.0000000000 |
| cmovbe | 0.0001314191 | 0.0000964306 | 0.0000026736 |
| cmove | 0.0030921788 | 0.0003939283 | 0.0000752610 |
| cmovg | 0.0001584909 | 0.0000240330 | 0.0000004247 |
| cmovge | 0.0000999755 | 0.0000000000 | 0.0000000000 |
| cmovl | 0.0000486198 | 0.0000094885 | 0.0000009475 |
| cmovle | 0.0001271497 | 0.0000041919 | 0.0000011607 |
| cmovne | 0.0017783231 | 0.0002729279 | 0.0000310218 |
| cmovns | 0.0001012792 | 0.0000981419 | 0.0000009787 |
| cmovs | 0.0000588429 | 0.0000258632 | 0.0000003125 |
| cmp | 0.1218090644 | 0.0000000000 | 0.0000000003 |
| cpuid | 0.0000073423 | 0.0000095105 | 0.0000537751 |
| cvtssi2sd | 0.0002406818 | 0.0000000000 | 0.0000000000 |
| cvtssi2ss | 0.0001036783 | 0.0000000000 | 0.0000000000 |
| cvttsd2si | 0.0000074056 | 0.0000000000 | 0.0000000000 |
| cvttss2si | 0.0000370280 | 0.0000000000 | 0.0000000000 |
| cwde | 0.0000000000 | 0.0000599484 | 0.0000029365 |
| dec | 0.0000000004 | 0.0002381938 | 0.0002023263 |
| div | 0.0000138980 | 0.0000022417 | 0.0014093084 |
| divsd | 0.00000765486 | 0.0000012175 | 0.0000002694 |
| divss | 0.0000074056 | 0.0000000000 | 0.0000000000 |
| enter | 0.0000000000 | 0.0000407058 | 0.0000029950 |
| fcmovnb | 0.0000000000 | 0.0000062804 | 0.0000001839 |

Continued on Next Page...

Table E.6 – Continued

| HMM Parameters | | | |
|-----------------------|--------------|--------------|--------------|
| fild | 0.0000005389 | 0.0000011504 | 0.0000167704 |
| fisttp | 0.0000002058 | 0.0000051380 | 0.0000567070 |
| fld | 0.0000074056 | 0.0000000000 | 0.0000000000 |
| fmul | 0.0000000000 | 0.0000184894 | 0.0000010865 |
| fstp | 0.0000041018 | 0.0000074992 | 0.0000008759 |
| fsub | 0.0000018514 | 0.0000000000 | 0.0000000000 |
| fucomp | 0.0000037028 | 0.0000000000 | 0.0000000000 |
| fxch | 0.0000037028 | 0.0000000000 | 0.0000000000 |
| hlt | 0.0000000000 | 0.0000787735 | 0.0000456841 |
| icebp | 0.0000000000 | 0.0000391792 | 0.0000020718 |
| idiv | 0.0000000000 | 0.0000063730 | 0.0002887542 |
| imul | 0.0006122794 | 0.0017069258 | 0.0011072843 |
| in | 0.0000088156 | 0.0000369855 | 0.0000029363 |
| inc | 0.0000978800 | 0.0000107109 | 0.0002825873 |
| ja | 0.0071982375 | 0.0000000000 | 0.0000000000 |
| jae | 0.0044896415 | 0.0000000000 | 0.0000000000 |
| jb | 0.0044266939 | 0.0000000001 | 0.0000000000 |
| jbe | 0.0060337079 | 0.0000000000 | 0.0000000000 |
| je | 0.1196614145 | 0.0000000316 | 0.0000000005 |
| jg | 0.0038620174 | 0.0000000000 | 0.0000000000 |
| jge | 0.0012977429 | 0.0000001003 | 0.0000000009 |
| jl | 0.0018939807 | 0.0000000000 | 0.0000000000 |
| jle | 0.0063077547 | 0.0000127123 | 0.0000000677 |
| jmp | 0.0644172341 | 0.0134160245 | 0.0715801504 |
| jne | 0.0695847451 | 0.0000000782 | 0.0000000024 |
| jnp | 0.0000037028 | 0.0000000000 | 0.0000000000 |
| jns | 0.0007647518 | 0.0003380045 | 0.0000049546 |
| jo | 0.0000001955 | 0.0000142735 | 0.0000006654 |
| jp | 0.0000111084 | 0.0000000000 | 0.0000000000 |
| js | 0.0031610721 | 0.0000264531 | 0.0000006679 |
| ldmxcsr | 0.0000092570 | 0.0000000000 | 0.0000000000 |
| lea | 0.0163598218 | 0.0486691714 | 0.0143699143 |
| leave | 0.0004008389 | 0.0000010553 | 0.0002951972 |
| lock | 0.0000006591 | 0.0000008555 | 0.0001208145 |
| lod | 0.0000000000 | 0.0000020111 | 0.0000001866 |
| loop | 0.0000000000 | 0.0000084117 | 0.0000001877 |
| loope | 0.0000002271 | 0.0000000000 | 0.0001488236 |
| loopne | 0.0000000000 | 0.0000641447 | 0.0000192646 |
| mov | 0.1835068386 | 0.6817903164 | 0.3080046846 |
| movabs | 0.0006096951 | 0.0002853643 | 0.0005383271 |
| movapd | 0.0000555396 | 0.0000000027 | 0.0000000000 |
| movaps | 0.0028141258 | 0.0000000000 | 0.0000000000 |
| movs | 0.0000000000 | 0.0001099191 | 0.0000307737 |
| movsd | 0.0000677987 | 0.0005323671 | 0.0003110500 |
| movss | 0.0000555420 | 0.0000000000 | 0.0000000000 |
| movsx | 0.0019932330 | 0.0006513406 | 0.0005616580 |
| movsxd | 0.0011773337 | 0.0251075494 | 0.0063304003 |
| movzx | 0.0252138044 | 0.0017584942 | 0.0054858204 |
| mul | 0.0000000000 | 0.0001081539 | 0.0000075057 |

Continued on Next Page...

Table E.6 – Continued

| HMM Parameters | | | |
|-----------------------|--------------|--------------|--------------|
| mulsd | 0.0000591981 | 0.0000000356 | 0.0000000277 |
| mulss | 0.0000444336 | 0.0000000000 | 0.0000000000 |
| neg | 0.0000958148 | 0.0003869207 | 0.0008204500 |
| nop | 0.0448083873 | 0.0111497760 | 0.0015285884 |
| not | 0.0001164287 | 0.0011825577 | 0.0027570567 |
| or | 0.0043755194 | 0.0019436983 | 0.0056111448 |
| out | 0.0000000007 | 0.0000242027 | 0.0000021314 |
| pop | 0.0396439971 | 0.0000000000 | 0.0000000000 |
| push | 0.0402901351 | 0.0000000000 | 0.0000000000 |
| rep | 0.0003720701 | 0.0012545017 | 0.0009346186 |
| repnz | 0.0000000000 | 0.0010618879 | 0.0003806675 |
| repz | 0.0051787613 | 0.0000000000 | 0.0000025438 |
| ret | 0.0204153817 | 0.0001521154 | 0.0004823938 |
| retf | 0.0000000000 | 0.0000020846 | 0.0000000748 |
| rex | 0.0000000000 | 0.0000001596 | 0.0000159770 |
| rol | 0.0000000000 | 0.0012890875 | 0.0001617761 |
| ror | 0.0000000000 | 0.0002182096 | 0.0002489281 |
| sar | 0.0000000000 | 0.0025773822 | 0.0011779151 |
| sbb | 0.0009545611 | 0.0008967517 | 0.0000037268 |
| seta | 0.0009942010 | 0.0000000000 | 0.0000000000 |
| setae | 0.0000333252 | 0.0000000000 | 0.0000000000 |
| setb | 0.0009312535 | 0.0000000000 | 0.0000000000 |
| setbe | 0.0000499878 | 0.0000000000 | 0.0000000000 |
| sete | 0.0034602637 | 0.0000000002 | 0.0000000000 |
| setg | 0.0002314230 | 0.0000000021 | 0.0000000000 |
| setge | 0.0000443831 | 0.0000000573 | 0.0000000013 |
| setl | 0.0001147867 | 0.0000000000 | 0.0000000000 |
| setle | 0.0000370280 | 0.0000000000 | 0.0000000000 |
| setne | 0.0028010475 | 0.0000001220 | 0.0000000220 |
| sets | 0.0000074056 | 0.0000000000 | 0.0000000000 |
| shl | 0.0000000080 | 0.0219096285 | 0.0064945917 |
| shr | 0.0006075657 | 0.0012384284 | 0.0066612662 |
| sldt | 0.0000018514 | 0.0000000000 | 0.0000000000 |
| stmxcsr | 0.0000092570 | 0.0000000000 | 0.0000000000 |
| stos | 0.0000570179 | 0.0000700050 | 0.0000466967 |
| sub | 0.0114616550 | 0.0201788585 | 0.0366383704 |
| subsd | 0.0000037028 | 0.0000000000 | 0.0000000000 |
| subss | 0.0000185140 | 0.0000000000 | 0.0000000000 |
| test | 0.1089427232 | 0.0000000001 | 0.0000471196 |
| ucomisd | 0.0000259196 | 0.0000000000 | 0.0000000000 |
| ucomiss | 0.0001055297 | 0.0000000000 | 0.0000000000 |
| xchg | 0.0041833547 | 0.0006868617 | 0.0001250157 |
| xor | 0.0182797050 | 0.0888314225 | 0.0569142674 |
| xorpd | 0.0000188458 | 0.0000161514 | 0.0000008157 |